Supplemental Data

Figure S1

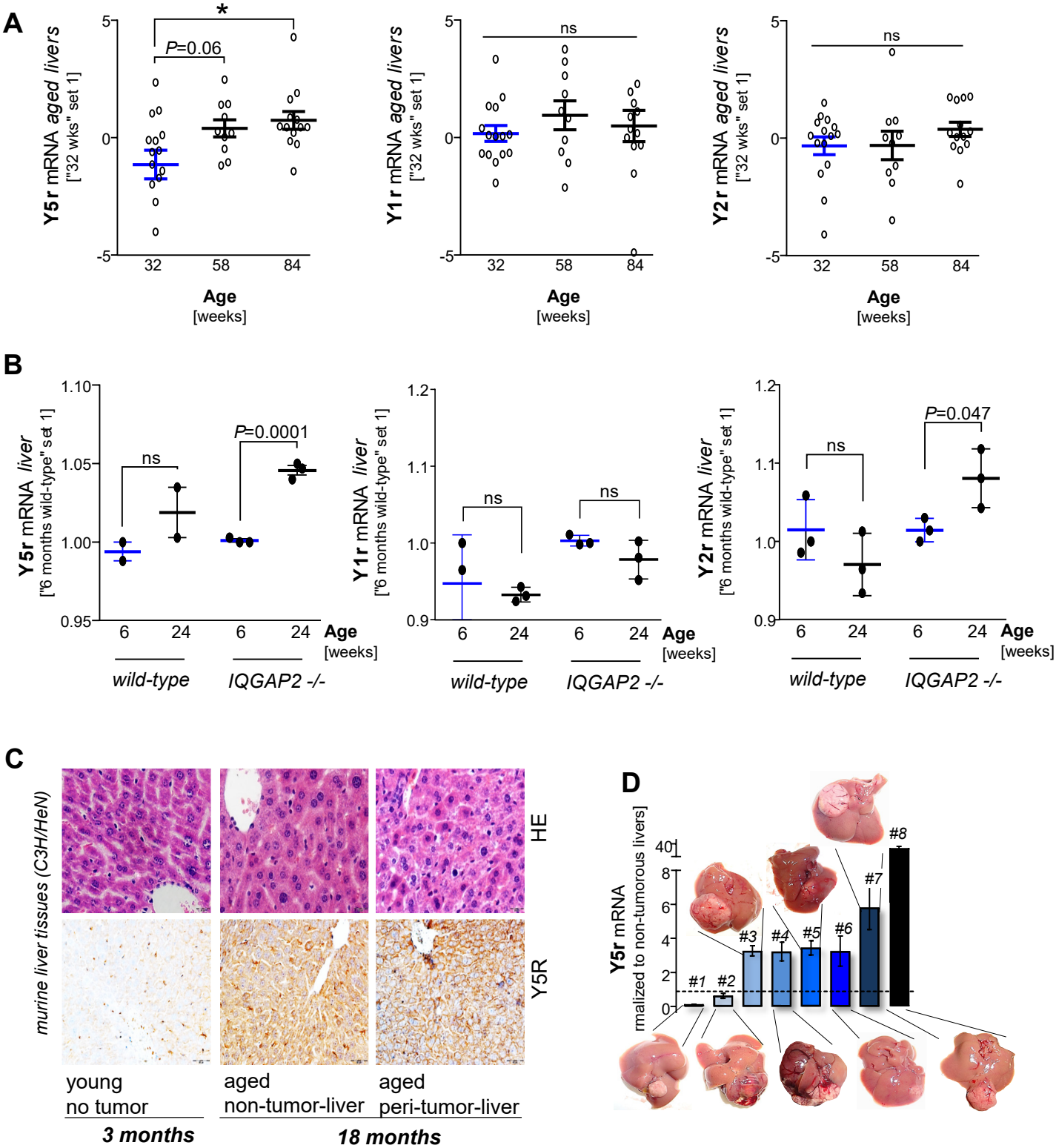

Figure S1. (related to Figure 1). **Age and cancer associated upregulation of Y5-receptor expression in a spontaneous mouse model of liver cancer and in patients with hepatocellular carcinoma.** (**A-B**) Gene Expression Omnibus (GEO) derived data of RNA expression levels of Npy-receptors (Y1r, Y2r, and Y5r) in liver tissues of mice and rats of different age. (A) Expression data (normalized expression value) of 32 (n = 15), 58 (n = 10) and 84 (n = 13) weeks old rats (GEO dataset "GDS2915"). (B) Normalized RNA expression levels in wild-type and IQGAP2-knockout (which are prone to HCC development) non-/pre-tumorous mouse livers at 6 and 24 weeks of age (n = 3) (GEO dataset "GDS4874"). Transcript profiling studies had identified the IQGAP2-knockout mouse model as a valid model for advanced human hepatocellular carcinoma (PMID: 23951254). (**C**) Representative images of Y5r protein expression (immunohistochemical analysis, 10-fold magnification) and paired HE-staining (20-fold magnification) in non-tumorous liver tissues of young (3 months) as compared to aged (18 months) non-tumor- and tumor-bearing C3H/HeN mice (n = 10). (**D**) Quantitative RT-PCR analysis of normalized Y5r mRNA levels in HCCs as compared to peri-tumorous liver tissues of aged (18 months) C3H/HeN mice (n = 8) (non-tumorous liver set 1). Data are presented as the mean ± SEM. Statistical significance was determined by ordinary one-way ANOVA together with Dunnett's multiple comparisons test (**A**), 2-tailed, unpaired t-test (**B**), 2-tailed, paired t-test (**D**). *P < 0.05, ns: non-significant.

Figure S1 *(continuation)*

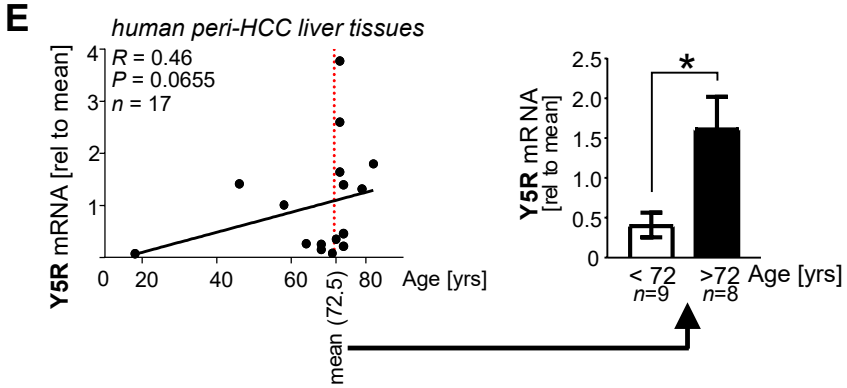

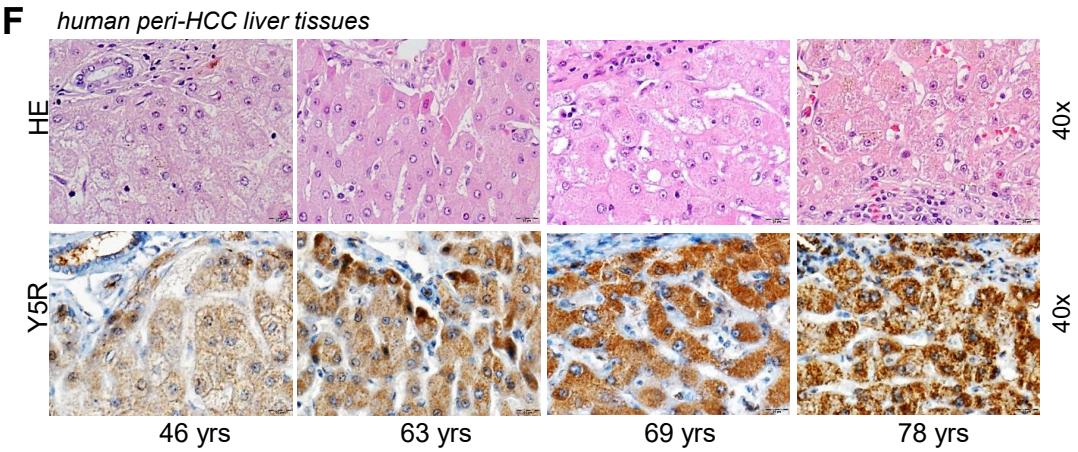

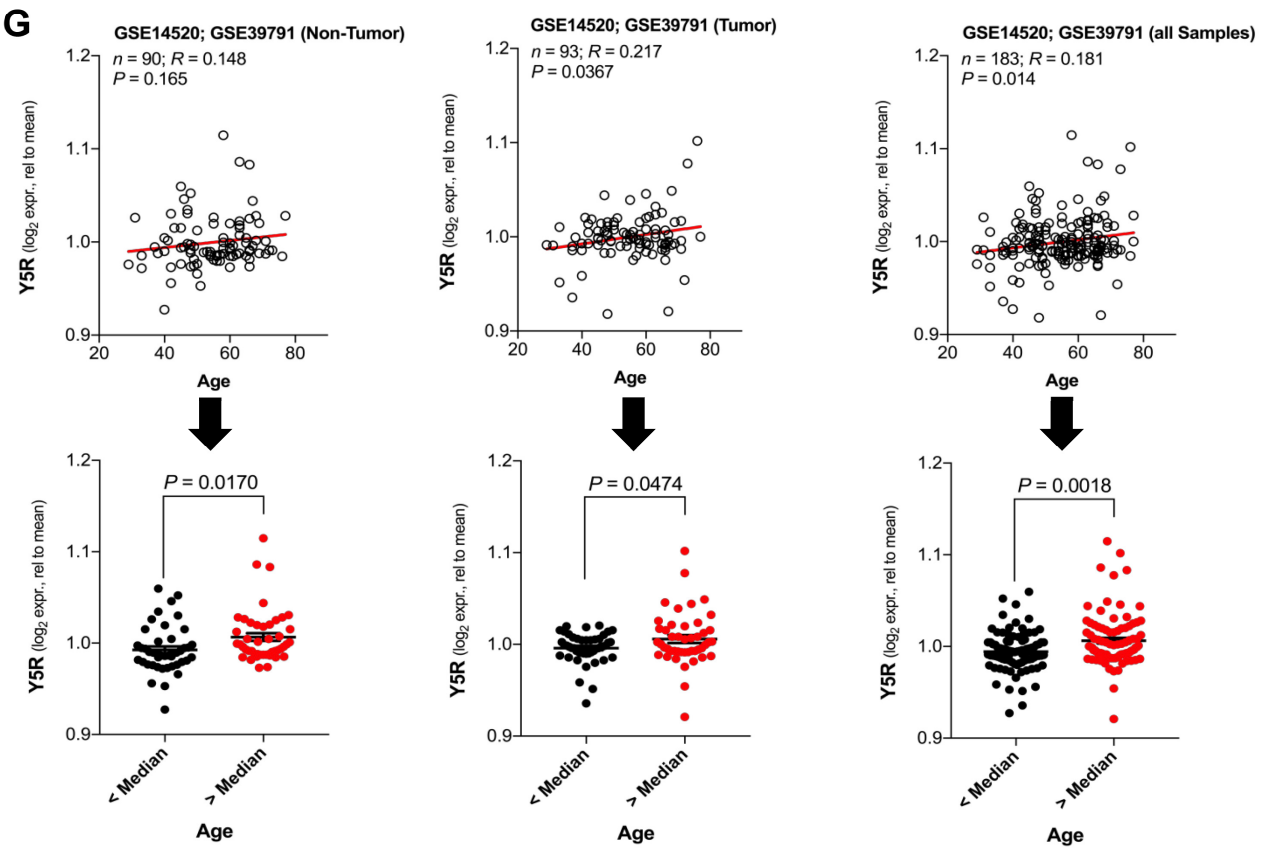

Figure S1 (related to Figure 1) (*continuation*). (**E**,**F**) Age-dependent Y5R mRNA analysis (qRT-PCR) (E) (n = 17) and representative images of immunostaining of Y5R and HE-staining (F) (n = 108) in human peri-tumorous liver tissues derived from HCC patients (20-fold magnification). (**G**) Tumor and non-tumor tissue samples derived from the datasets GSE14520 and GSE39791 were used. The expression data (log_2) of each dataset were shown as normalized to the mean. The panels reveal Y5R expression in non-tumorous (left, n = 90), tumorous (center, n = 93) and summarized non-tumorous and tumorous liver tissue samples (right, n = 183). Y5R expression is depicted as correlated with age (upper panels) as well as in young (i.e. age < median age of each cohort) compared with aged (i.e. age > median of each cohort) patient groups (lower panels). Data are presented as the mean ± SEM. Statistical significance was determined by 2-tailed, unpaired t-test (**E**,**G**) and Pearson correlation (**E**,**G**). To determine the effect of the age on the expression of Y5R we also used a linear regression model (**G**). *P < 0.05.

Figure S1 *(continuation)*

H

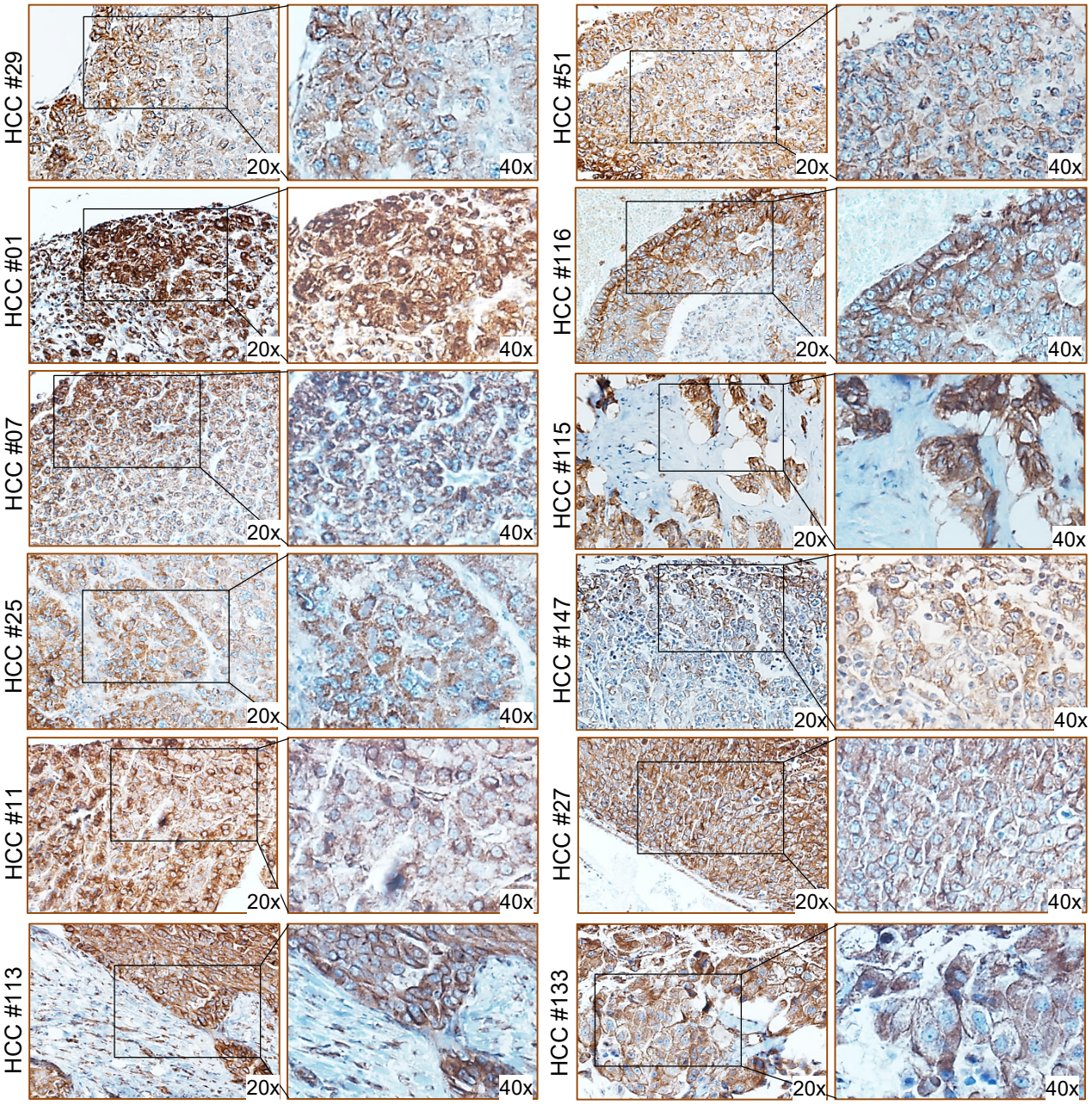

I

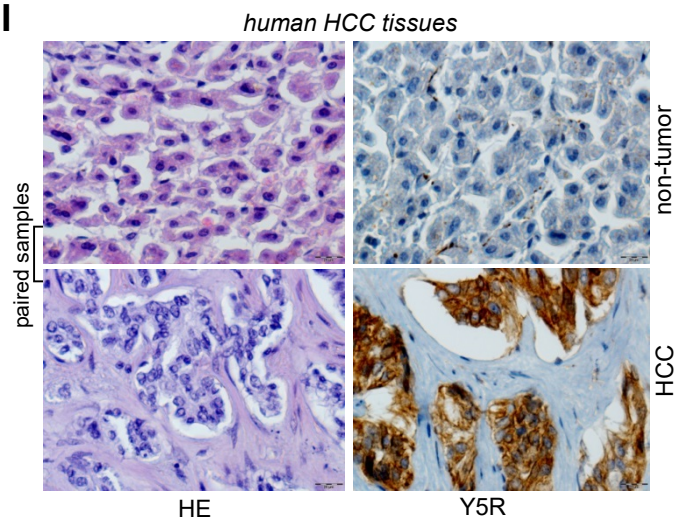

Figure S1 (related to Figure 1) (*continuation*). (**H**,**I**) Representative images of Y5R protein staining in different human HCC samples (H) (*n* = 230) (20- and 40-fold magnifications, respectively) and representative paired HCC and peri-tumorous liver tissue (I) derived from a tissue micro array (20-fold magnification) (*n* = 230) .

Figure S1 *(continuation)*

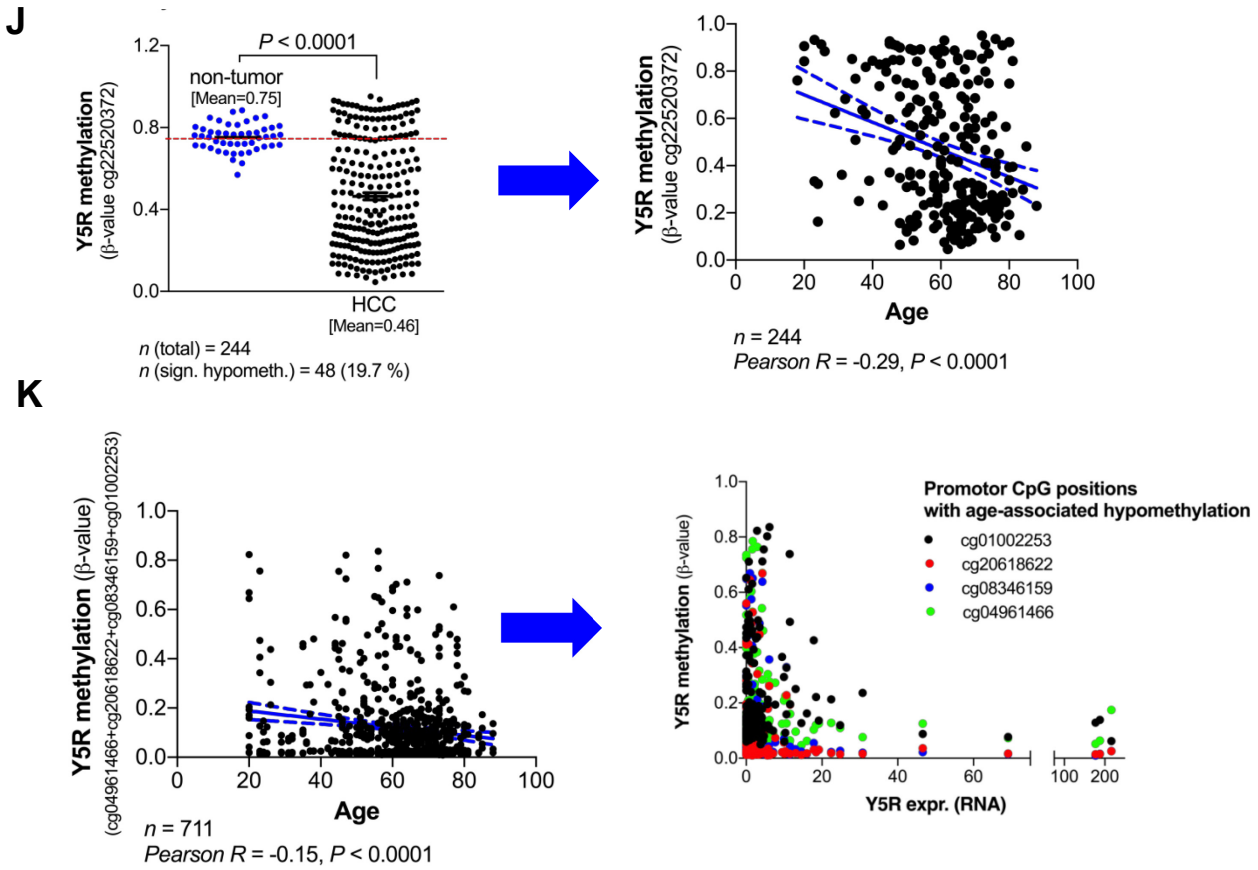

Figure S1 (related to Figure 1) (*continuation*). (**J**) Y5R CpG methylation (probe position: cg22520372, gene body) (*n* = 244) in HCC as compared to non-HCC tissues (*left panel*) and as correlated with age (*right panel*) as determined in TCGA data applying the Catalogue of Somatic Mutations in Cancer (COSMIC) database. (**K**) *Left panel*: Summarized Y5R CpG methylation of four promotor sites (probe positions: cg04961466, cg20618622, cg08346159, cg01002253) (*n* = 722) in HCC tissues as correlated with age. The respective positions as depicted were selected because of significant correlation of methylation patterns and age. *Right panel*: Y5R expression (gene expression value was obtained from RNA Seq RPKM (Reads Per Kilobase per Million mapped reads) values (TCGA Data Portal) as correlated with Y5R methylation (beta value for measuring methylation level ranging from 0 (least methylated) to 1 (most methylated). The respective positions as depicted (one gene body site and four promotor sites) were selected because of significant correlation of methylation patterns and age. Age- and cancer-associated differential methylation is commonly found in HCC and other cancer types and can drive cancer progression (Perez et al. Aging Cell. 2018 Jun;17(3):e12744; Mudbhary et al. Cancer Cell. 2014 Feb 10;25(2):196-209; Argemi et al. Nat Commun. 2019 Jul 16;10(1):3126; Bárcena-Varela et al. Hepatology. 2019 Feb;69(2):587-603). DNA methylation data were obtained from Illumina Infinium Human Methylation450 Beadchip from the TCGA Data Portal of different sites: promotor (position/probes: cg15586439 | cg13975625 | cg11784623 | cg21748223 | cg01002253 | cg04961466 | cg20618622 | cg08346159 | cg1034115) (I), 200 base pair (bp) region at transcription start site (TSS) (position/probes: cg01002253 | cg04961466 | cg20618622 | cg08346159) (J) and CpG-island (positiion/probes: cg11784623 | cg21748223 | cg01002253 | cg04961466 | cg20618622 | cg08346159 | cg10341154 | cg18438777) (*n* = 231). Data were analyzed applying the Catalogue of Somatic Mutations in Cancer (COSMIC) database and the MethHC database (MethHC: a database of DNA methylation and gene expression in human cancer. W.Y. Huang, S.D. Hsu, H.Y. Huang, Y.M. Sun, C.H. Chou, S.L. Weng, H.D. Huang*. Nucleic Acids Res. 2015 Jan;43(Database issue):D856-61). Statistical significance was determined by or 2-tailed, unpaired t-test (left panel of (**J**)) and by Pearson correlation (right panel of (**J**), **K**).

Figure S1 *(continuation)*

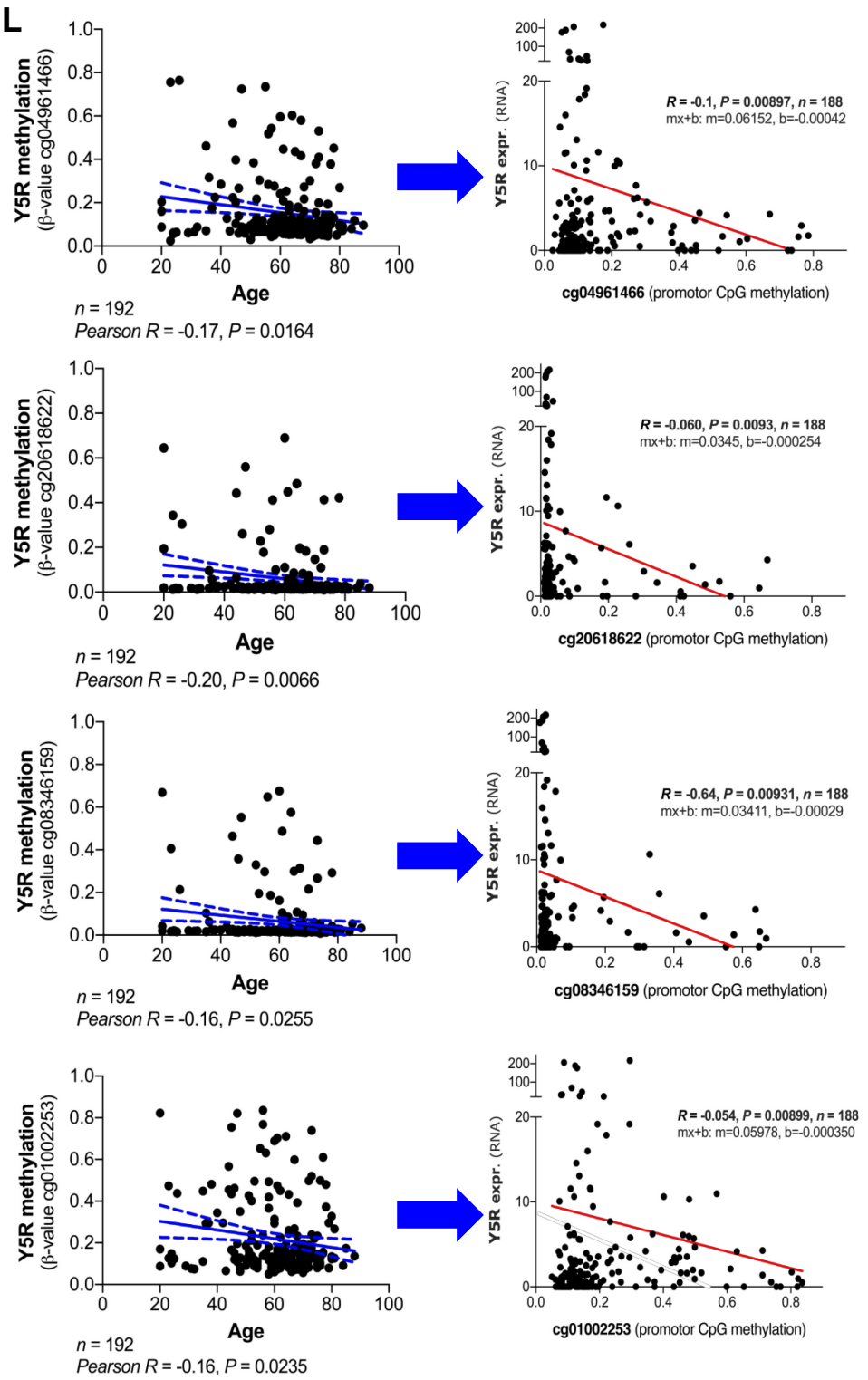

Figure S1 (related to Figure 1) (*continuation*). (**L**) *Left panels*: Y5R CpG methylation of each promotor site (probe positions: cg04961466, cg20618622, cg08346159, cg01002253) (*n* = 192) in HCC tissues as correlated with age. The respective positions as depicted (promotor regions) were selected because of significant correlation of methylation patterns and age. *Right panels*: Y5R expression (gene expression value was obtained from RNA Seq RPKM (Reads Per Kilobase per Million mapped reads) values (TCGA Data Portal) as correlated with Y5R methylation (beta value for measuring methylation level ranging from 0 (least methylated) to 1 (most methylated). Together, these data link age-related hypomethylation of several Y5R promotor sites with Y5R expression levels. Reduced promotor hypomethylation patterns in aged as compared with younger patients are negatively correlated with Y5R expression, thereby potentially inducing Y5R in older patients. Data were obtained applying the Catalogue of Somatic Mutations in Cancer (COSMIC) database and the MethHC database (MethHC: a database of DNA methylation and gene expression in human cancer. W.Y. Huang, S.D. Hsu, H.Y. Huang, Y.M. Sun, C.H. Chou, S.L. Weng, H.D. Huang*. Nucleic Acids Res. 2015 Jan;43(Database issue):D856-61). Statistical significance was determined by Pearson correlation.

Figure S2

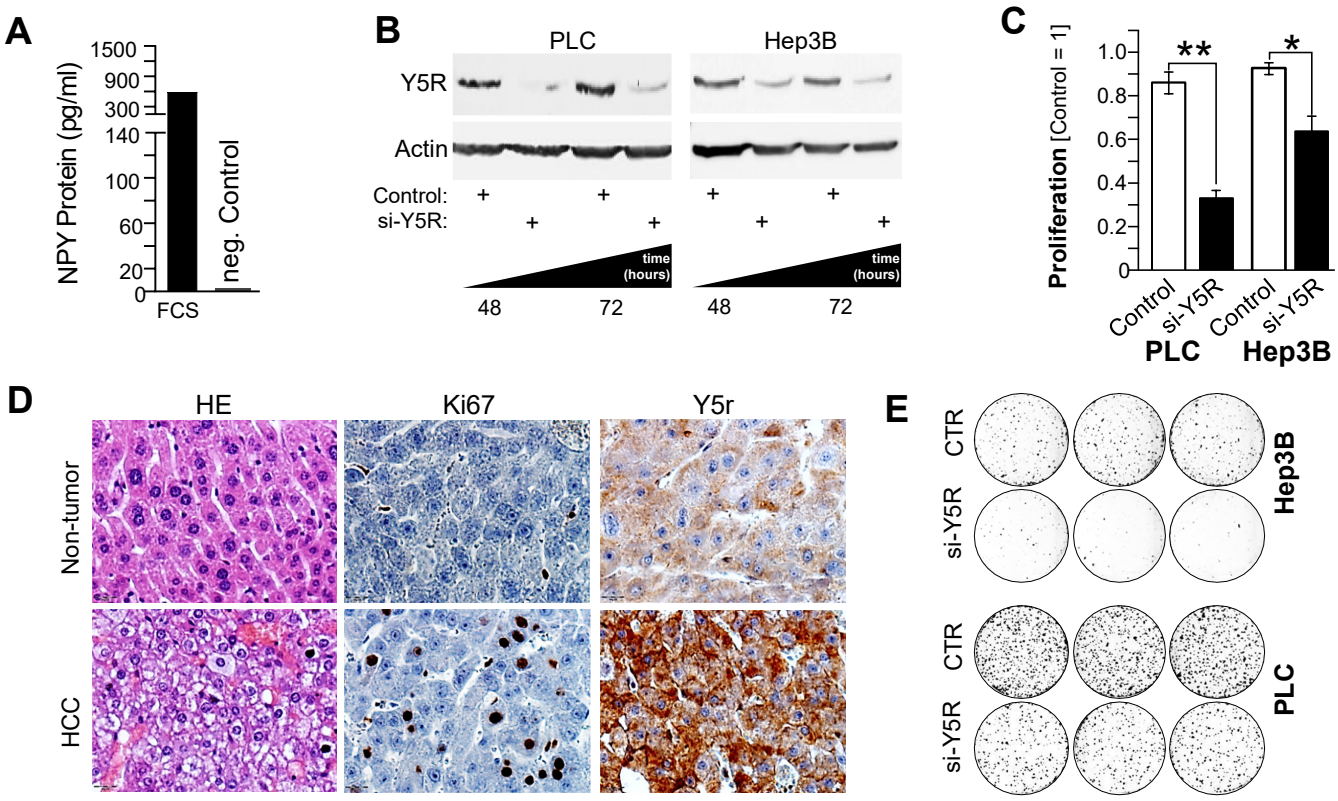

Figure S2 (related to Figure 2)**. Y5R enhances tumorigenicity of HCC and correlates with tumor progression and poor survival.** (**A**) Enzyme-linked immunosorbent assay (ELISA)-analysis of NPY protein levels in fetal calf serum (FCS) (supplemented to cell culture medium) and in serum-free medium (neg. Control) (*n* = 2). (**B**) Representative Western blot analysis of Y5R expression in HCC cells (PLC, Hep3B) using si-RNA-pool-mediated knockdown (e.g. 48 and 72 h after transfection) (*n* = 3). (**C**) Real-time cell proliferation (xCELLigence) analysis of HCC cells (PLC, Hep3B) after RNAi-mediated knockdown of Y5R as compared to control-transfected cells (*n* = 3). (**D**) Representative HE and immunostaining (Ki67, Y5r) (20-fold magnification) of paired age-related HCC and peri-tumorous liver tissues derived from C3H/HeN mice (*n* = 8). (**E**) Clonogenic assays (representative images of three replicates) of control-transfected and si-Y5R-transfected HCC cells (PLC, Hep3B) (*n* = 3). Data are presented as the mean ± SEM. Statistical significance was determined 2-tailed, unpaired t-test (**C**). **P* < 0.05, ***P* < 0.01.

Figure S2 *(continuation)*

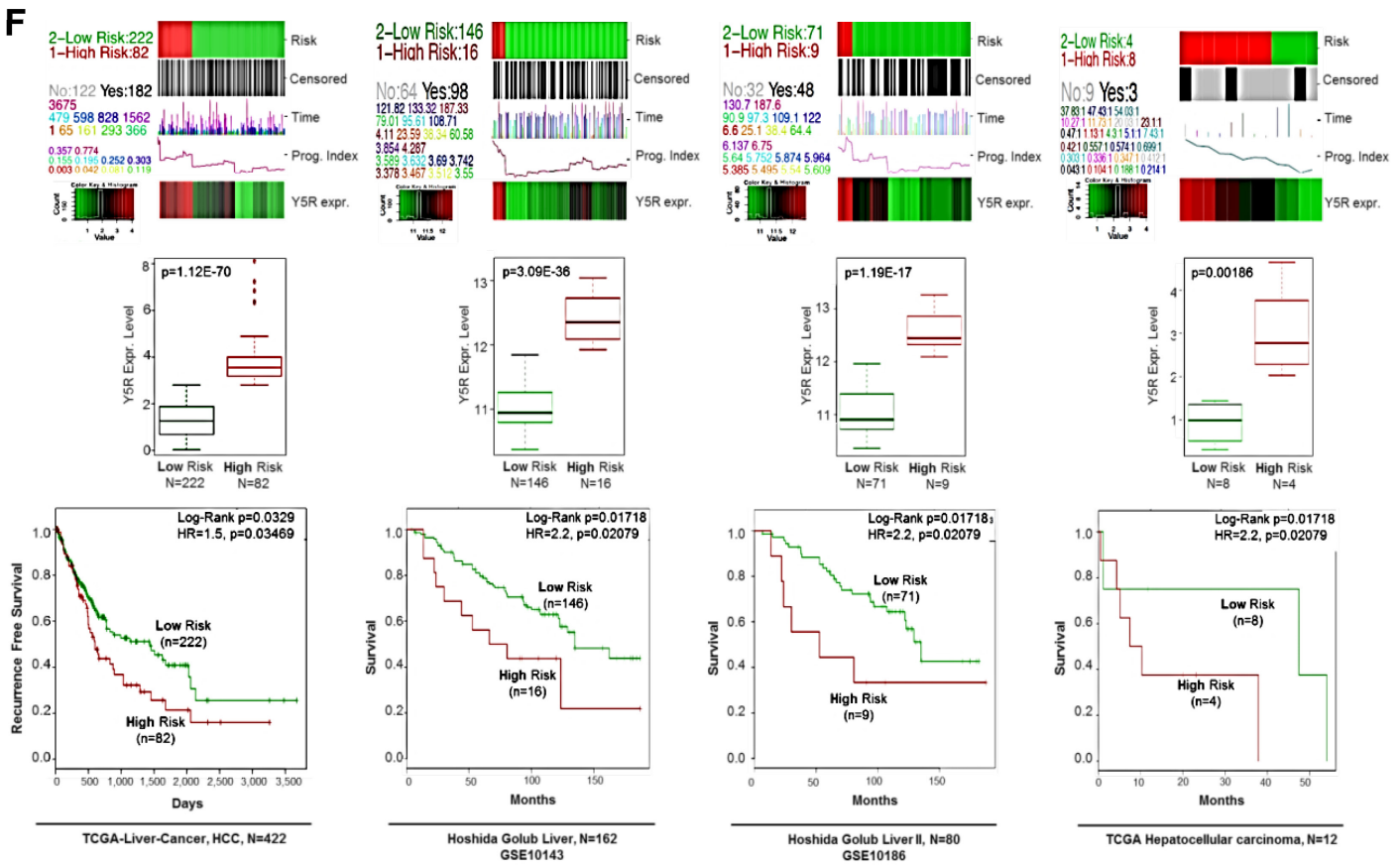

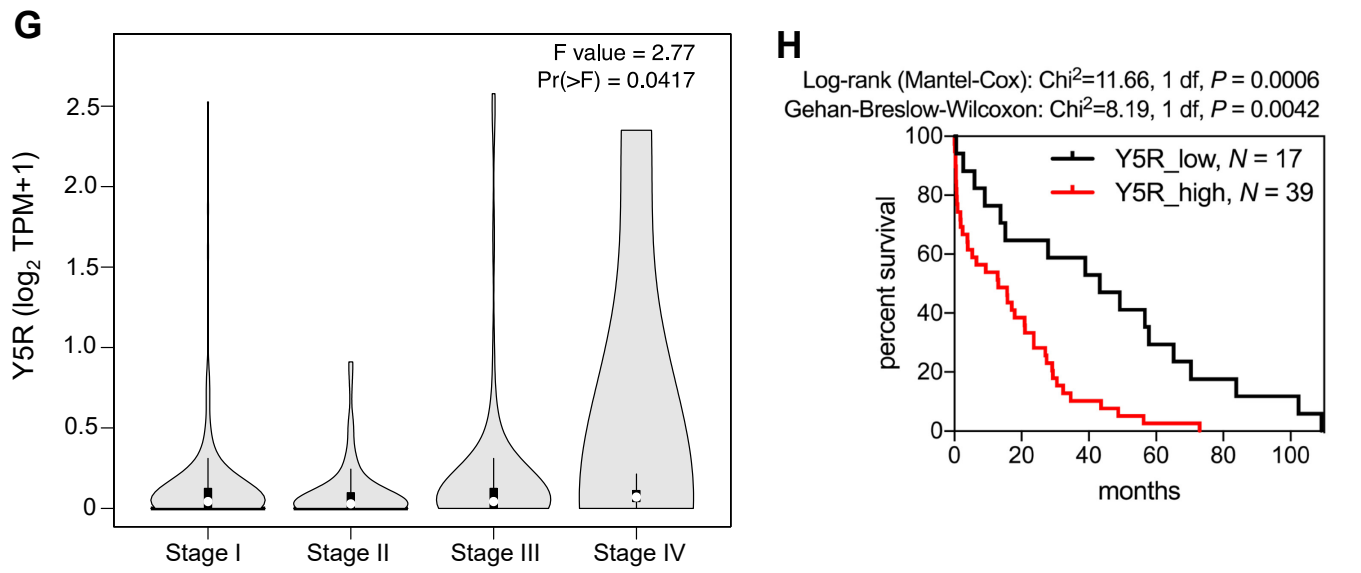

Figure S2 (related to Figure 2) (*continuation*). (**F**) "SurvExpress-Biomarker validation for cancer gene expression" database analysis of Y5R expression and according Kaplan-Meier curve for overall survival in several TCGA- and GSE-derived datasets. Computational stratification into "low risk" and "high risk" patient groups was based on prognostic index ("HR": Hazard ratio). The numbers of patients in groups (*n*) and *P*-values are depicted within the panels. (**G**) Stage plot of NPY5R expression levels in different tumor stages of HCC patients (TCGA dataset analysis) applying the Gene Expression Profiling Interactive Analysis (GEPIA) database (http://gepia.cancer-pku.cn/index.html) (Tang, Z. et al. (2017) GEPIA: a web server for cancer and normal gene expression profiling and interactive analyses. Nucleic Acids Res, 10.1093/nar/gkx247). The expression data are first $\log_2$(TPM+1) transformed for differential analysis. (**H**) According Kaplan-Meier curve for patient survival (as depicted in Figure 2H) applying a tissue micro array. Statistical significance was determined by computational log-rank testing and Hazard ratios (**F**,**H**). The method for differential gene expression analysis (**G**) was one-way ANOVA, using pathological stage as variable for calculating differential expression: Gene expression ~ pathological stage.

Figure S3

A

Y5-NPY-receptor inhibitors

Official Name	*Abbreviation*	*Ki (Y5R, nM)*	*Ki (Y1R, nM)*	*Ki (Y2R, nM)*	*Ki (Y4R, nM)*	*Ref.*
CGP 71683	Y5R-Inh#1	1.4	2765.0	7187.0	5637.0	**PMID**: 9854049
MK-0557	Y5R-Inh#2	1.6	*>7.500 fold*	*>7.500 fold*	*>7.500 fold*	**PMID**: 12145156
5RA972	Y5R-Inh#3	3.1	*>10.000 fold*	*>10.000 fold*	*>10.000 fold*	**PMID**: 17011500
S-2367 (Velneperit)	Y5R-Inh#4	*N/S*	*N/S*	*N/S*	*N/S*	**DOI:** 10.1021/acs.oprd.5b00023

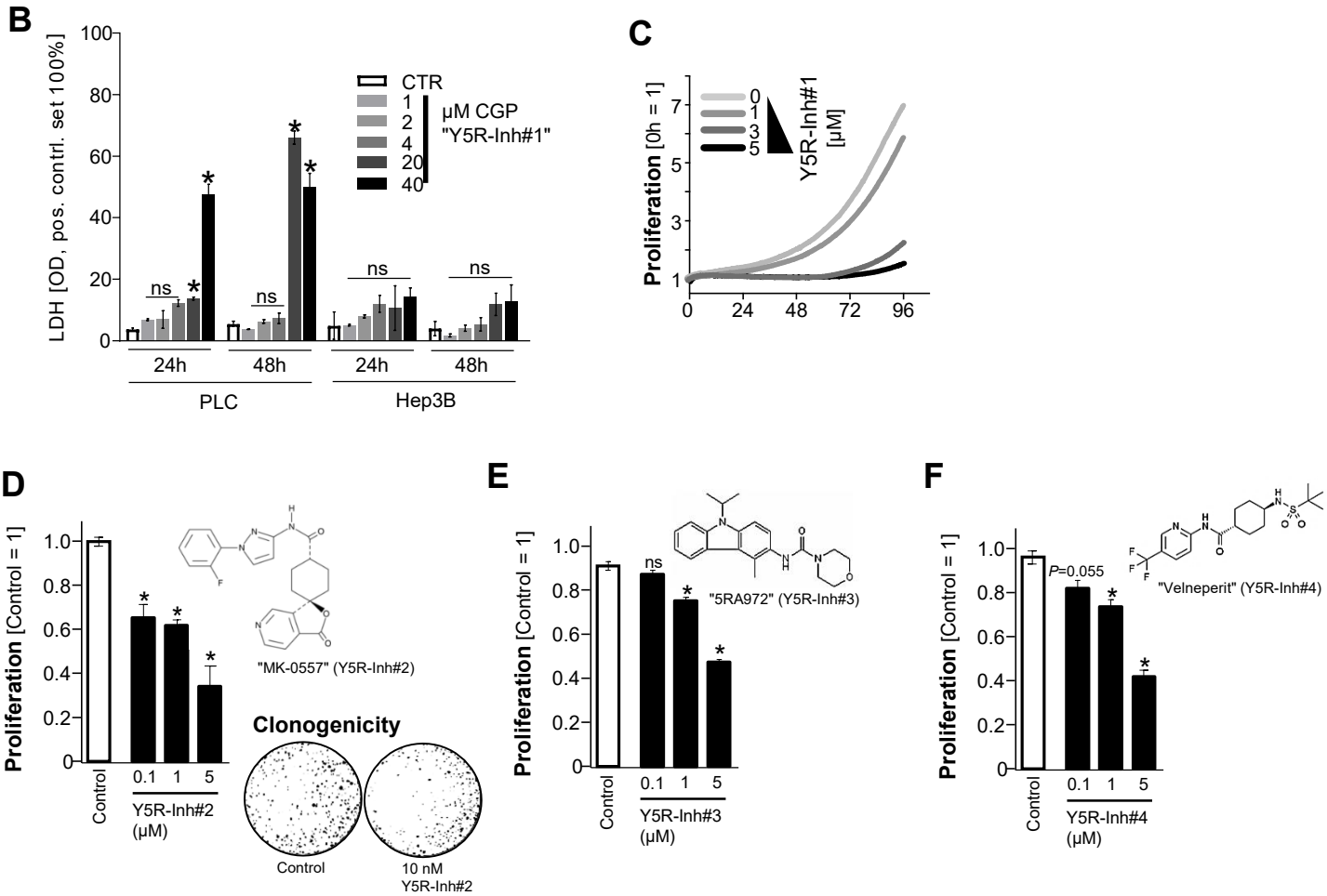

Figure S3 (related to Figure 3). (**A**) The table summarizes abbreviations, Ki-values and representative references (PMIDs, DOI) of the four different specific small molecule Y5R-inhibitors that were used in this study. CGP71683 was the inhibitor with the highest affinity for Y5R and was selected for in vivo analysis of Y5-receptor-inhibition. (**B**) Lactate dehydrogenase (LDH) activity (optic density (OD)) as analyzed in supernatants of HCC cell lines (PLC, Hep3B) (compared with control) after treatment with different doses of the specific Y5R-inhibitor (Y5R-Inh#1) (0, 1, 2, 4, 20, 40 µM) for 24 or 48 hours, respectively (n = 3). (**C**) Representative real-time proliferation curves of HCC cells (PLC) (xCELLigence) that were treated with different doses of Y5R-Inh#1 (0, 1, 3, 5 µM) (n = 3). (**D-F**) Real-time cell proliferation (xCELLigence) analysis of HCC cell lines (e.g. PLC) that were treated with different doses (0.1, 1, 5 µM) of Y5R-Inh#2 (D), Y5R-Inh#3 (E) and Y5R-Inh#4 (F) (n = 3). (D) also depicts representative images of a clonogenicity assay of Y5R-Inh#2-treated (10 nM) HCC cells (Hep3B) as compared to controls (n = 2). Moreover, the chemical formula of the specific Y5R-inhibitors are depicted. Data are presented as the mean ± SEM. Statistical significance was determined by ordinary one-way ANOVA together with Dunnett's multiple comparisons test. *P < 0.05 (as compared with the respective controls), ns: non-significant (as compared with the respective controls).

Figure S3 *(continuation)*

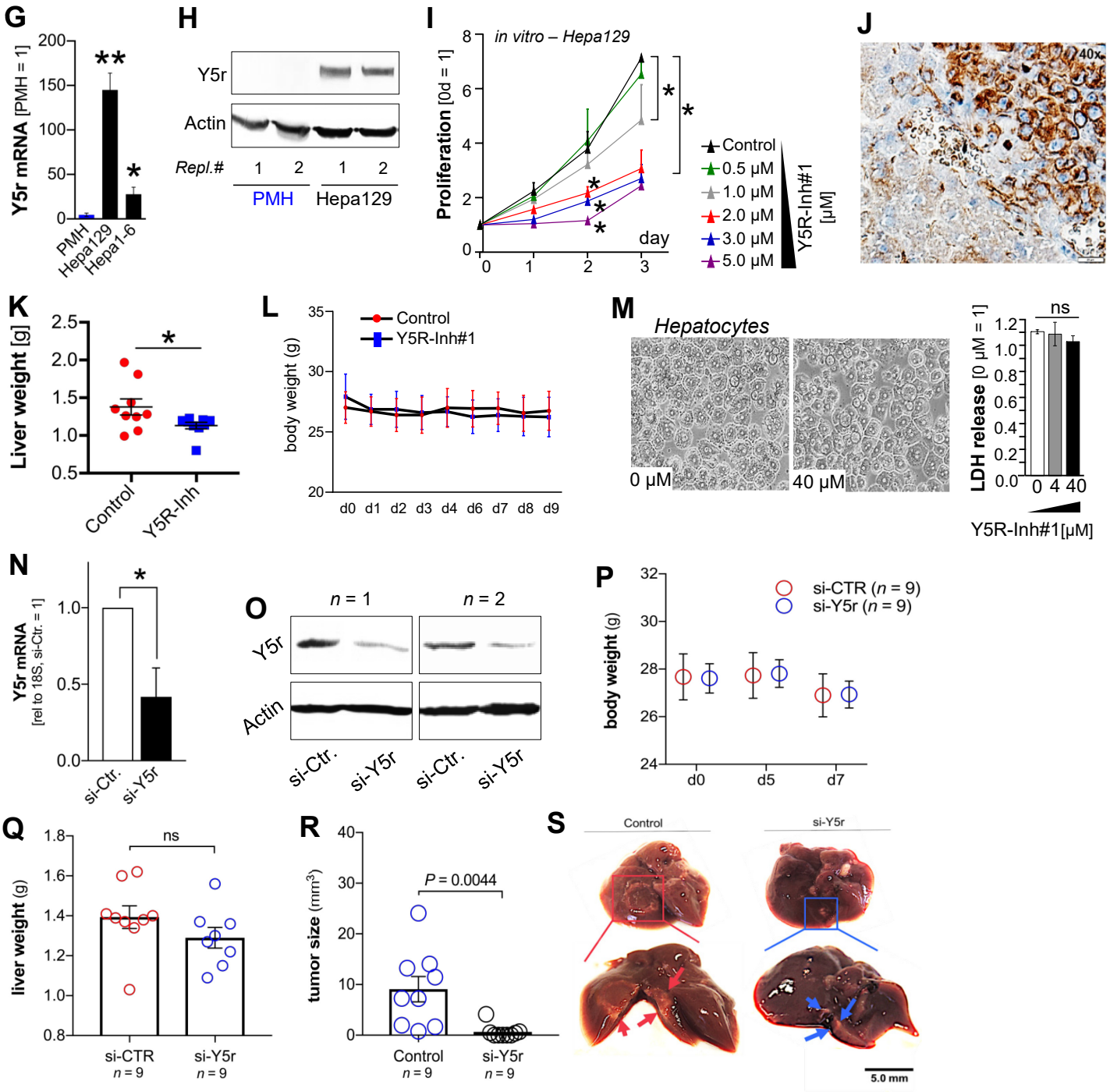

Figure S3 (related to Figure 3) (*continuation*). (**G**) Y5r mRNA levels (qRT-PCR analysis) of murine HCC cells (Hepa129, Hepa1-6) as compared with primary murine hepatocytes (PMH) (n = 3). (**H**) Western blot analysis of Y5r protein levels (representative image depicting n = 2 biological replicates of PMH and murine Hepa129 HCC cells). (**I**) Proliferation (normalized cell counts) of Hepa129 cells in vitro after treatment with different doses of Y5R-Inh#1 as compared to control-treated cells (n = 2). (**J**) Representative images (immunohistochemistry) of Y5r protein expression (40-fold magnification) in tissue samples containing HCC and surrounding non-tumorous liver tissue (orthotopic HCC mouse model) (n = 10). (**K**) Liver weights of mice that were treated with Y5R-Inh#1 (15 mg/KG b.w.) (n = 13) or control-treated (DMSO) (n = 13) applying the orthotopic HCC model. (**L**,**M**) No signs of toxic side effects applying pharmacologic Y5R-inhibition *in vivo (*using the specific small molecule Y5R-inhibitor CGP7168): (L) Body weights of mice treated with Y5R-Inh#1 (15 mg/KG b.w.) (n = 13) or control-treated (DMSO) (n = 13) applying the orthotopic HCC model. (M) Representative images (20-fold magnification) and LDH activity (optic density (OD)) as analyzed in supernatants of primary human hepatocytes (PHH) after treatment with different doses of the specific Y5R-inhibitor (Y5R-Inh#1) (0, 4, 40 µM) for 48 hours revealed no toxic effects of pharmacologic Y5R-inhibition on human hepatocytes (n = 3). (**N-S**) Hepa129 cells were transfected with pooled si-RNAs (two specific si-RNAs were combined to increase efficacy and reduced off-target effects) targeting Y5r (si-Y5r) (n = 9) or with control-si-RNAs (n = 9) for 48 hours before orthotopic HCC cell implantation was performed. Tumor volumes and emergence ("tumor") or absence ("no tumor") of macroscopic tumors was assessed after one week. Quantitative RT-PCR (N) (n = 3) and Western blot analysis (representative images of two biological replicates) (O) of si-RNA-mediated knockdown of Y5r in Hepa129. Body- (P) and liver- (Q) weights as well as tumor sizes (R) and representative images (S). Data are presented as the mean ± SEM. Statistical significance was determined by ordinary one-way ANOVA together with Dunnett's multiple comparisons test (**G,I,L,P**) or 2-tailed, unpaired t-test (**K,N,Q,R**). *P < 0.05 (as compared with the respective controls), ns: non-significant (as compared with the respective controls).

Figure S4

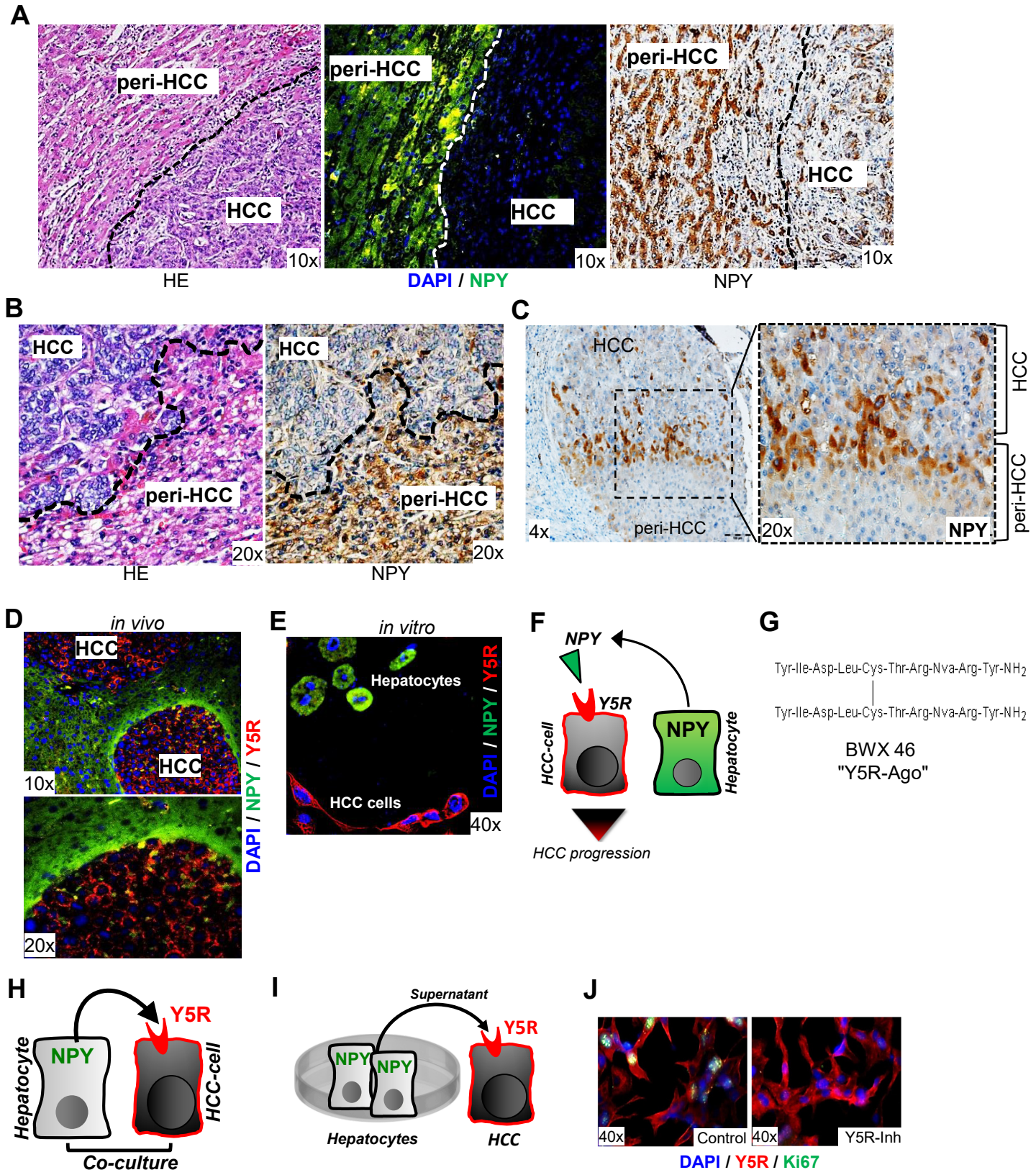

Figure S4 (related to Figures 4 and 5). **Neuropeptide Y is secreted by peri-tumorous hepatocytes and cross-talks with Y5-receptor in HCC.** (**A-C**) Representative images depicting HE-staining and NPY-immunostaining of HCC and peri-tumorous liver tissues ("peri-HCC") of human specimens (n = 115). (**D**,**E**) Representative images depicting co-immunostaining (immunofluorescence analysis) of Y5r (red) and Npy (green) applying (D) tissue samples derived from the orthotopic HCC mouse model (n = 10) and (E) co-culture experiments using hepatocytes (primary murine hepatocytes) and HCC cells (Hepa1-6) (n = 3). (**F**) Hypothesis of NPY-Y5R-crosstalk between hepatocytes and HCC cells: Peri-tumorous, hepatocyte-derived NPY induces Y5-receptor activation on HCC cells thereby affecting HCC progression. (**G**) Chemical formula/structure of the synthetic and highly specific Y5-receptor agonist BWX46 ("Y5R-Ago"). (**H**,**I**) Schemes of experimental design: Treatment of HCC-hepatocyte co-cultures (H) and treatment HCC cells with cell culture supernatant of (NPY-producing) hepatocytes (I). (**J**) Representative (co-)immunofluorescence (n = 2) of Y5r (red) and Ki67 (green) in control- and Y5R-inhibitor-treated HCC cells.

Figure S5

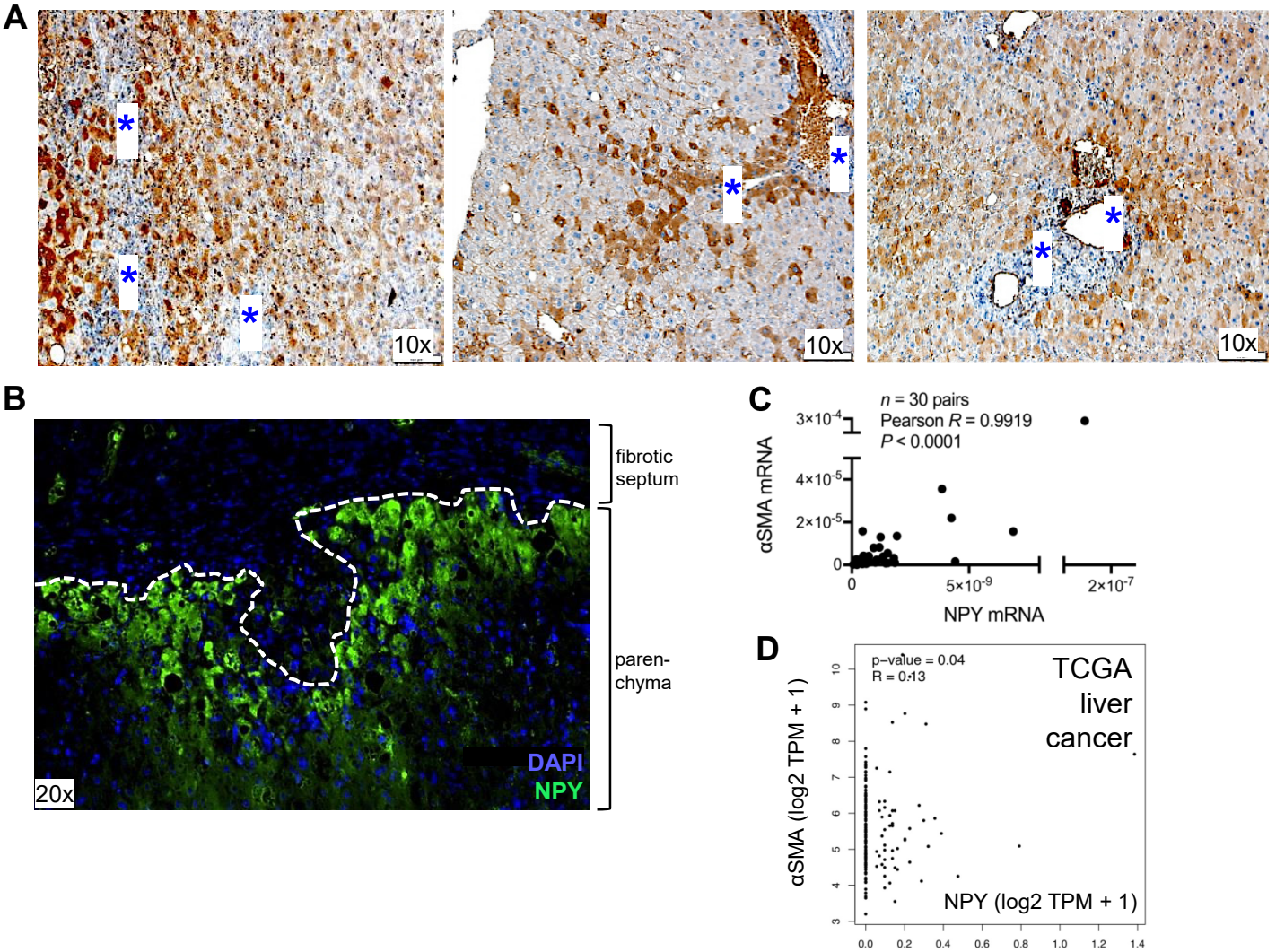

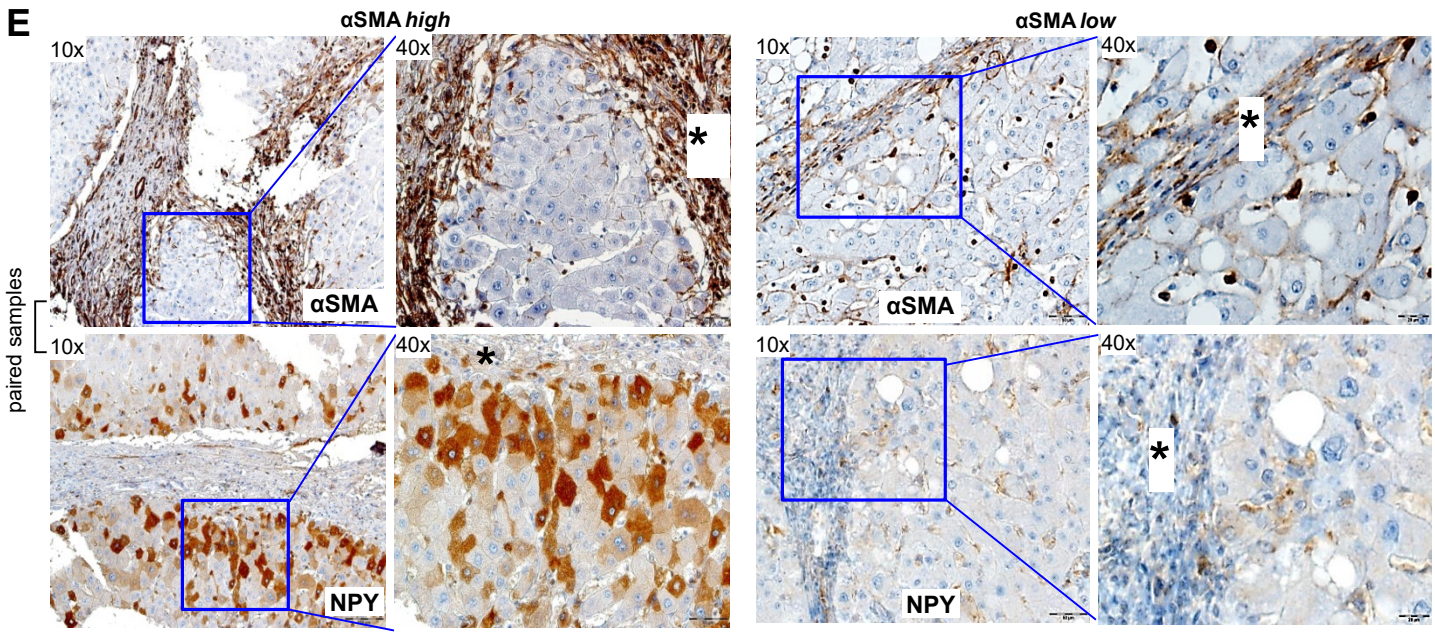

Figure S5 (related to Figure 6). **Peri-tumorous NPY expression is induced by hepatic fibrosis and stellate-cell activation.** (**A-B**) Immunohistochemistry (A) and immunofluorescence (B) analysis depicting NPY-staining (representative images of human peri-tumorous liver tissue applying a tissue micro array) (*n* = 115), revealing that NPY-immunopositive hepatocytes are mainly localized close to portal tracts and/or fibrotic septa (*). (**C**) Paired NPY and αSMA mRNA expression (qRT-PCR) analysis in human peri-tumorous liver tissues (*n* = 30). (**D**) Correlation of NPY and αSMA expression levels in HCC patients (TCGA dataset analysis) applying the Gene Expression Profiling Interactive Analysis (GEPIA) database (http://gepia.cancer-pku.cn/index.html) (Tang, Z. et al. (2017) GEPIA: a web server for cancer and normal gene expression profiling and interactive analyses. Nucleic Acids Res, 10.1093/nar/gkx247). Non-log scale was used for calculation and the log-scale axis ist used for visualization. (**E**) Immunohistochemical analysis applying human peri-tumorous liver tissue samples. Representative images are shown for NPY-staining in paired tissue samples with high as compared to low αSMA-expression (*: portal tracts and/or fibrotic septa) (*n* = 91 paired samples). Statistical significance was determined by Pearson correlation (**C**,**D**).

Figure S6

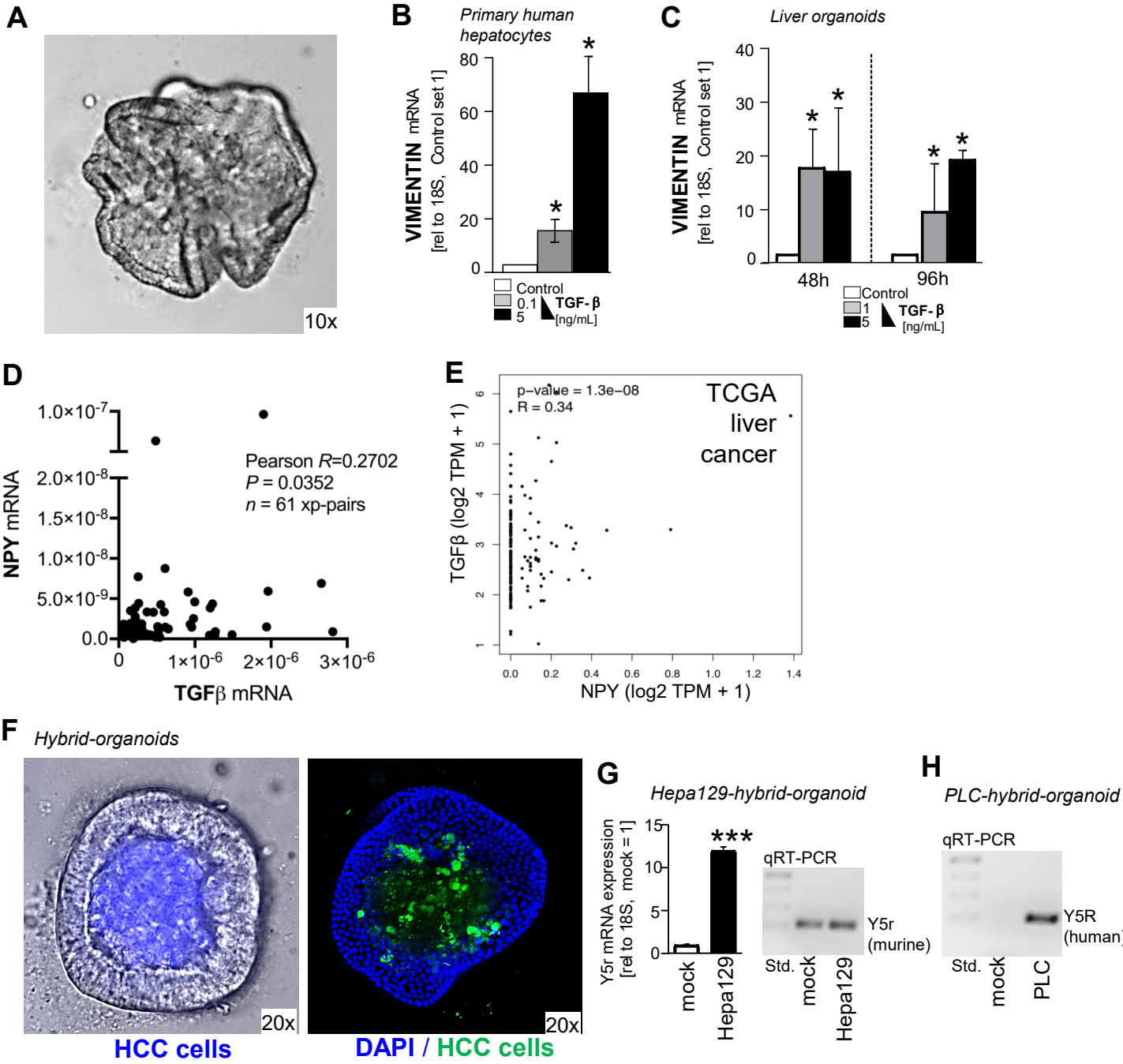

Figure S6 (related to Figure 7). (**A**) Representative image showing a liver organoid used as an additional model (next to primary human hepatocytes) to analyze NPY expression in hepatocytes (n = 6). Briefly, isolated embryonic liver cells (hepatoblasts) were embedded in Matrigel and covered with basal medium (HepatiCult™ Organoid Growth Medium (Mouse)) to initially form cysts that develop into liver organoids. (**B**,**C**) Quantitative RT-PCR analysis of Vimentin mRNA expression levels in TGFβ1-treated cultured primary human hepatocytes (PHH) (48 hours) (B) and in hepatoblast-derived liver organoids representing a three-dimensional model of differentiated hepatocytes (C) (n = 3). Vimentin represents a standard marker of EMT and established target gene of TGFβ1 in hepatocytes. (**D**) Correlated NPY and TGFβ mRNA expression and correlation analysis (qRT-PCR) applying human liver/HCC tissue samples (n = 61). (**E**) Correlation of NPY and TGFβ expression levels in HCC patients (TCGA dataset analysis) applying the Gene Expression Profiling Interactive Analysis (GEPIA) database (http://gepia.cancer-pku.cn/index.html) (Tang, Z. et al. (2017) GEPIA: a web server for cancer and normal gene expression profiling and interactive analyses. Nucleic Acids Res, 10.1093/nar/gkx247). Non-log scale was used for calculation and the log-scale axis ist used for visualization. (**F**) Establishment of a three-dimensional model hybrid-system to explore direct interaction of HCC cells and surrounding hepatocytes. Representative immunofluorescence images are depicted for murine HCC cells (Hepa129, labeled in blue) (left image) and human HCC cells (PLC, labeled in green) (right image) after implantation into hepatocyte-derived liver organoids using microinjection technique (HCC cells were labeled before implantation using CFSE) (n = 3). (**G**) Quantitative RT-PCR analysis of (murine) Y5r in liver organoids that consist of hepatocytes only (mock) as compared to hybrid-organoids that consist of murine HCC cells (Hepa129) surrounded by hepatocytes reveals that Y5r is mainly expressed by HCC cells (n = 3). (**H**) PCR analysis of (human) Y5r in liver organoids that consist of hepatocytes only (mock) as compared to hybrid-organoids that consist of human HCC cells (PLC) surrounded by hepatocytes reveals that Y5R is strongly expressed by HCC cells also in this model system (n = 3). Data are presented as the mean ± SEM. Statistical significance was determined by 2-tailed, unpaired t-test (**G**), ordinary one-way ANOVA together with Dunnett's multiple comparisons test (**B,C**) or Pearson correlation (**D**,**E**). *P < 0.05, ***P < 0.001 (as compared with control and mock, respectively).

Figure S6 *(continuation)*

I

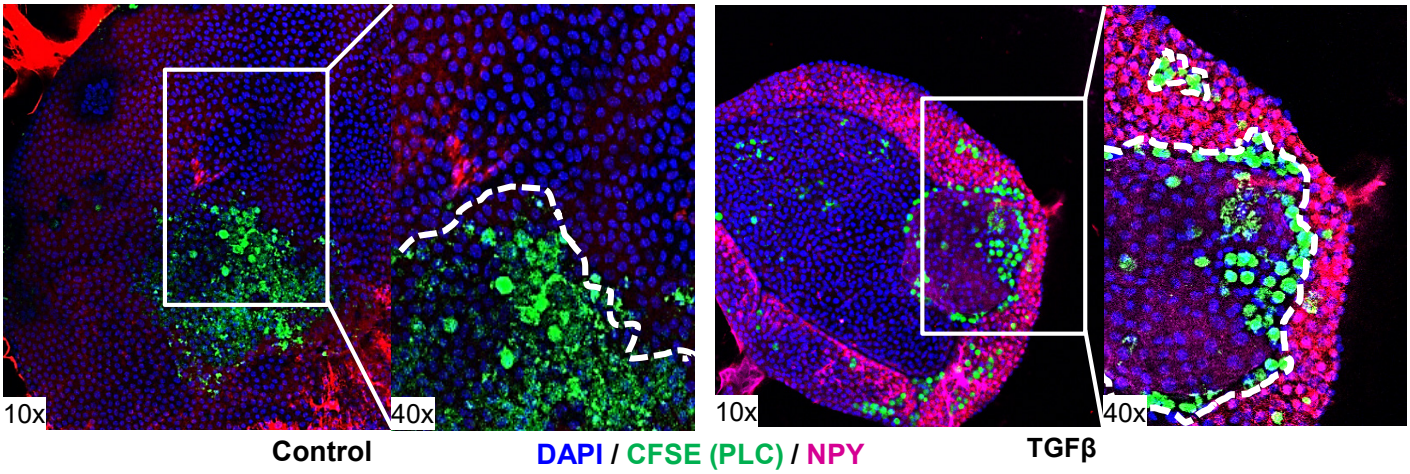

J

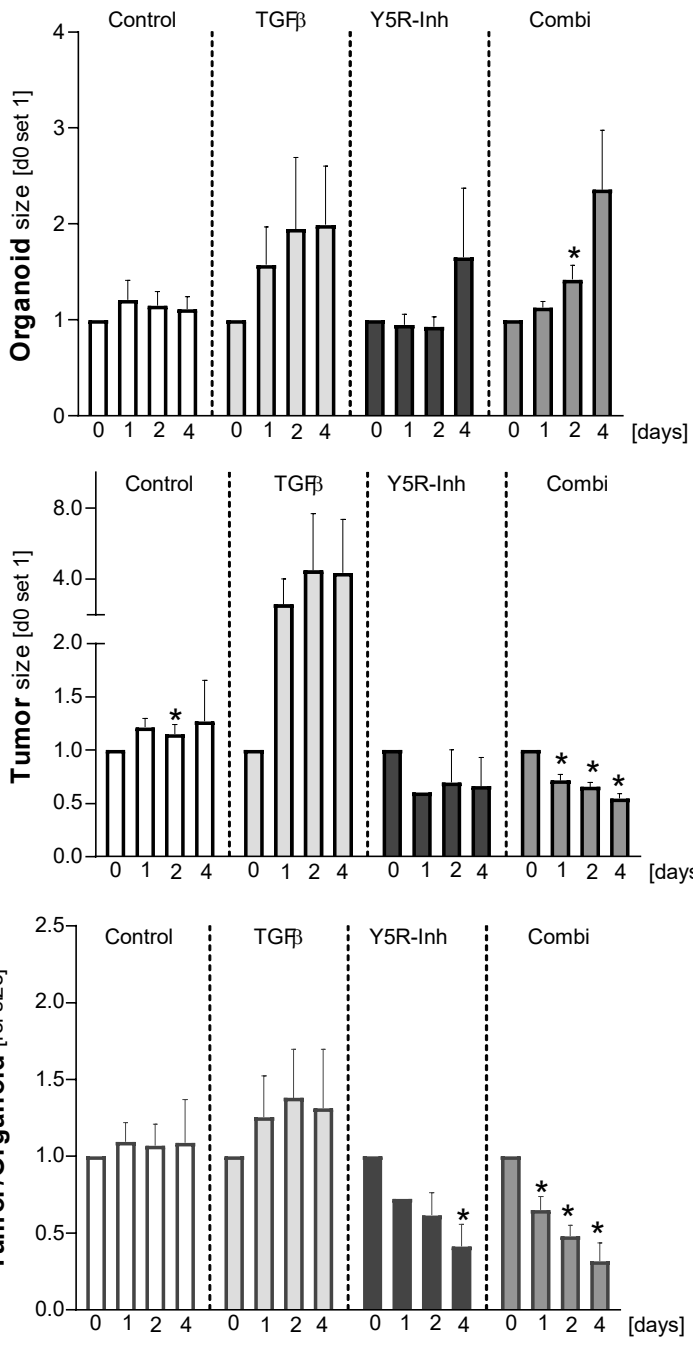

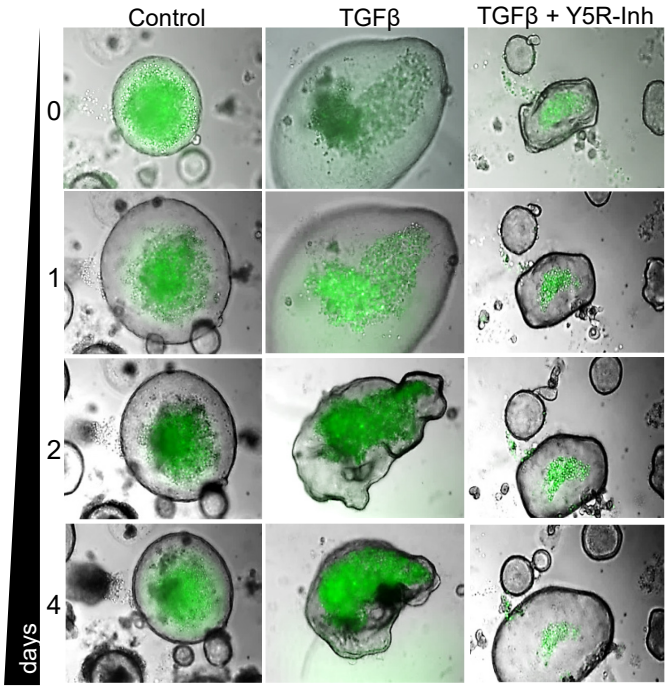

Figure S6 (related to Figure 7) (*continuation*). (**I**) Representative confocal immunofluorescence images of hybrid-organoids (PLC cells surrounded by hepatocytes) shows that TGFβ1-treatment induces NPY expression by hepatocytes surrounding the HCC cells (PLC) (n = 2; 4 replicates). (**J**) Normalized (compared to day 0) sizes of hybrid-organoids (upper panel), micro-injected tumor cells (center), and the ratios of tumor/organoid (bottom panel) as well as representative images (HCC cells labeled with CFSE (green)) (10-fold magnification). The hybrid-organoids were control-treated or treated with TGFβ1, Y5R-Inh#1, or a combination of TGFβ1 and Y5R-Inh#1 (combi). TGFβ1-treatment enhanced growth of both organoids and implanted tumors. In contrast, co-treatment with TGFβ1 and Y5R-Inh#1 rescued the growth-enhancing effects of TGFβ on HCC cells (without affecting the organoids), resulting in a strong reduction of tumor-to-organoid-size ratios (n = 2; 4 replicates). Data are presented as the mean ± SEM. Statistical significance was determined by ordinary one-way ANOVA together with Dunnett's multiple comparisons test. *P < 0.05 as compared with the respective control (i.e. 0 days) (**J**).

Figure S7

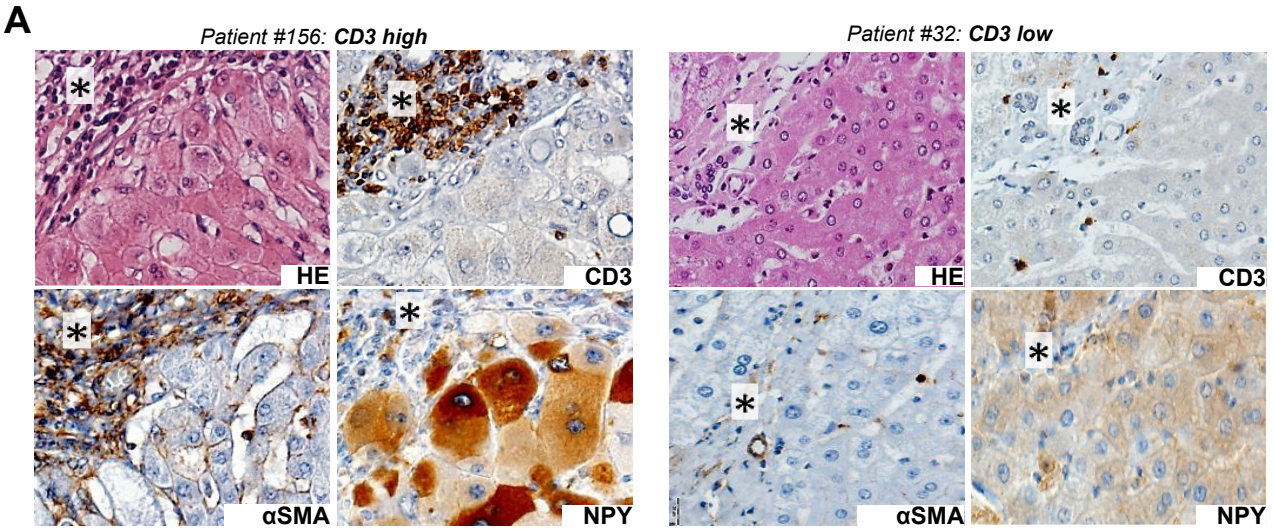

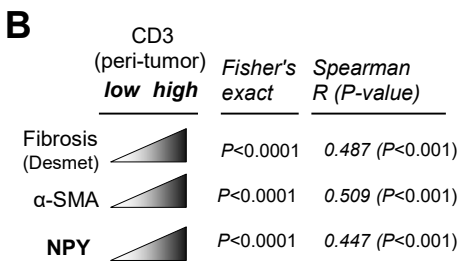

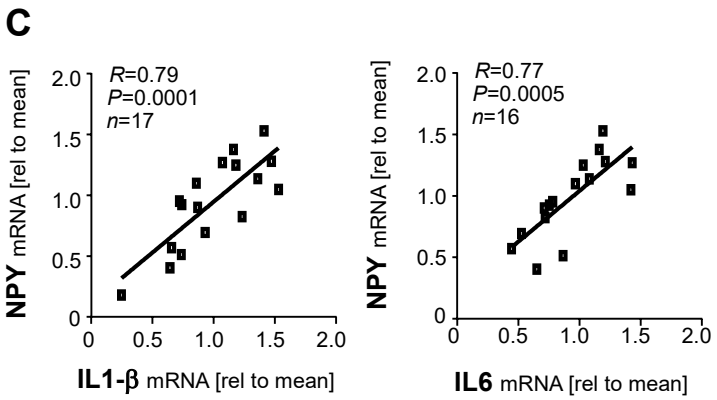

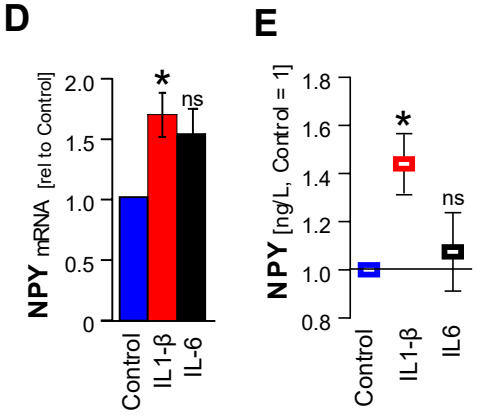

Figure S7 (related to Figure 7) (*continuation*). (**A,B**) Immunohistochemical analysis applying human peri-tumorous liver tissue samples. Representative images (40-fold magnification) are shown for HE-, αSMA-, and NPY-staining in paired/corresponding tissue samples with high as compared to low CD3-expression (*: portal tracts and/or fibrotic septa). (B) depicts statistics including Fisher's exact and Spearman correlation values of fibrosis score (n = 91), peri-tumorous αSMA-staining (n = 87), peri-tumorous NPY-staining (n = 102), and survival (n = 56) of HCC patients with high as compared with low CD3-staining (see also Table S5). (**C**) Correlated NPY and IL-1β (n = 17) or NPY and IL-6 (n = 16), respectively, mRNA expression (qRT-PCR) analysis in human peri-tumorous liver tissues. (**D**,**E**) Normalized NPY mRNA levels as quantified by qRT-PCR (P), and normalized NPY protein levels in cell supernatants as quantified by ELISA of hepatocytes that were treated with IL-1β or IL-6, respectively, for 48 hours, as compared with control-treated cells. Data are presented as the mean ± SEM. Statistical significance was determined by two-sided Fisher's exact test and Spearman correlation (**B**), Pearson correlation (**C**), and by 2-tailed, unpaired t-test (**D**,**E**). *P < 0.05, ns: non-significant (as compared with control).

Figure S8

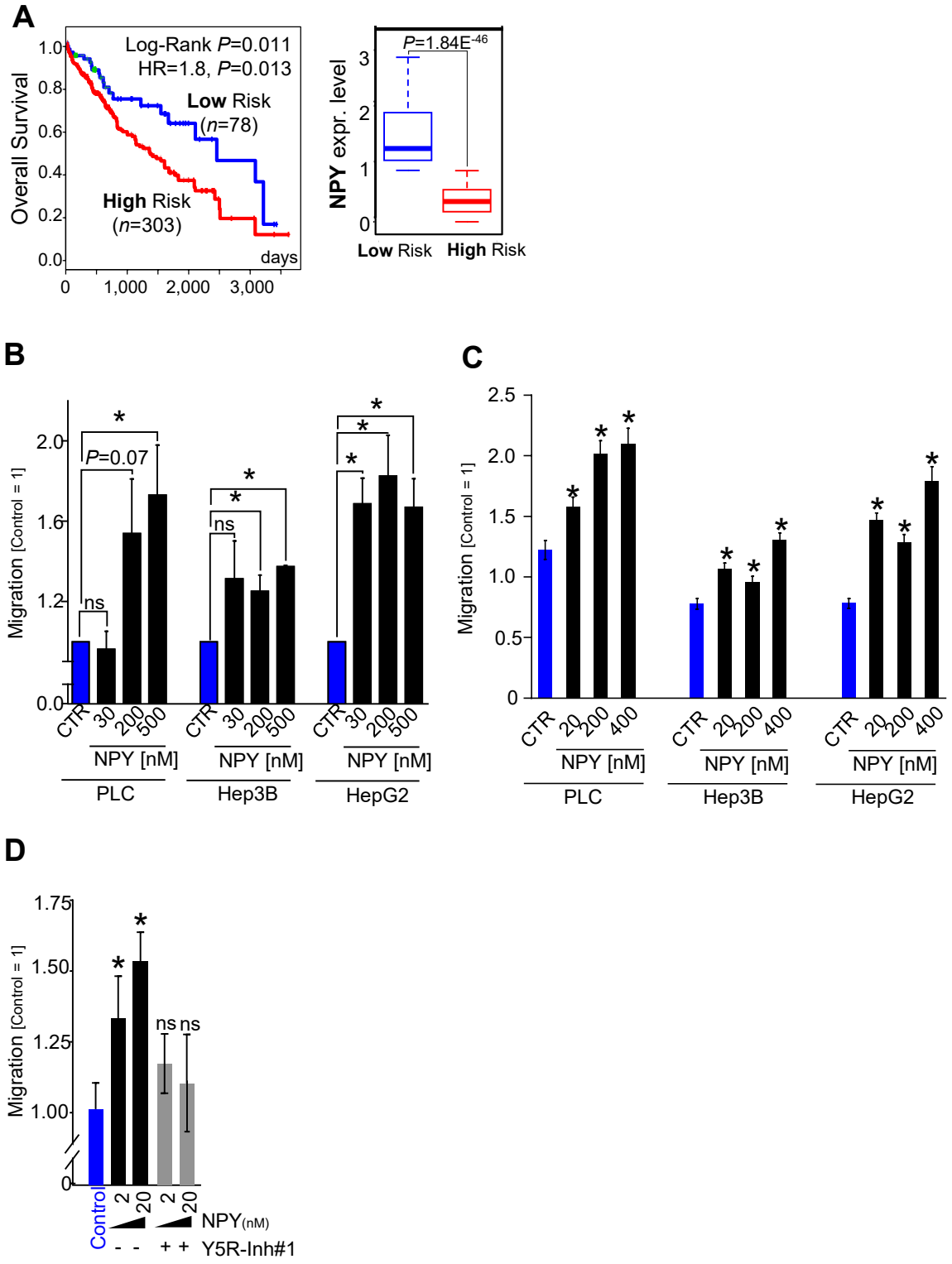

Figure S8 (related to Figure 8). **Hepatocyte-derived NPY mediates chemotaxis *via* activation of Y5R and Y5R and NPY are strongly expressed at sites of stroma-invasion and promote invasion of HCC cells.** (**A**) "SurvExpress-Biomarker validation for cancer gene expression" database analysis of NPY expression and according Kaplan-Meier curve for overall survival in a TCGA-derived dataset. Computational stratification into "low risk" and "high risk" patient groups was based on prognostic index ("HR": Hazard ratio). (**B**,**C**) Real-time cell migration (xCELLigence) (n = 3) (B) and Boyden chamber migration (n = 3) (C) analysis of different human HCC cell lines (PLC, Hep3B, HepG2) towards a chemotactic gradient induced by different doses of recombinant NPY that was supplemented to the lower chambers as compared to controls (CTR) (*P < 0.05 *vs.* control. ns: non-significant *vs.* control). (**D**) Boyden chamber cell migration assay of HCC cells (Hepa129) towards a chemotactic gradient induced by different doses of recombinant NPY that was supplemented to the lower chambers with or without co-treatment with Y5R-Inh#1, as compared to controls (CTR) (*P < 0.05 *vs.* control. ns: non-significant *vs.* control) (n = 3). Data are presented as the mean ± SEM. Statistical significance was determined by computational log-rank testing and Hazard ratio (**A**) and by ordinary one-way ANOVA together with Dunnett's multiple comparisons test (**B**,**C**,**D**).

Figure S9

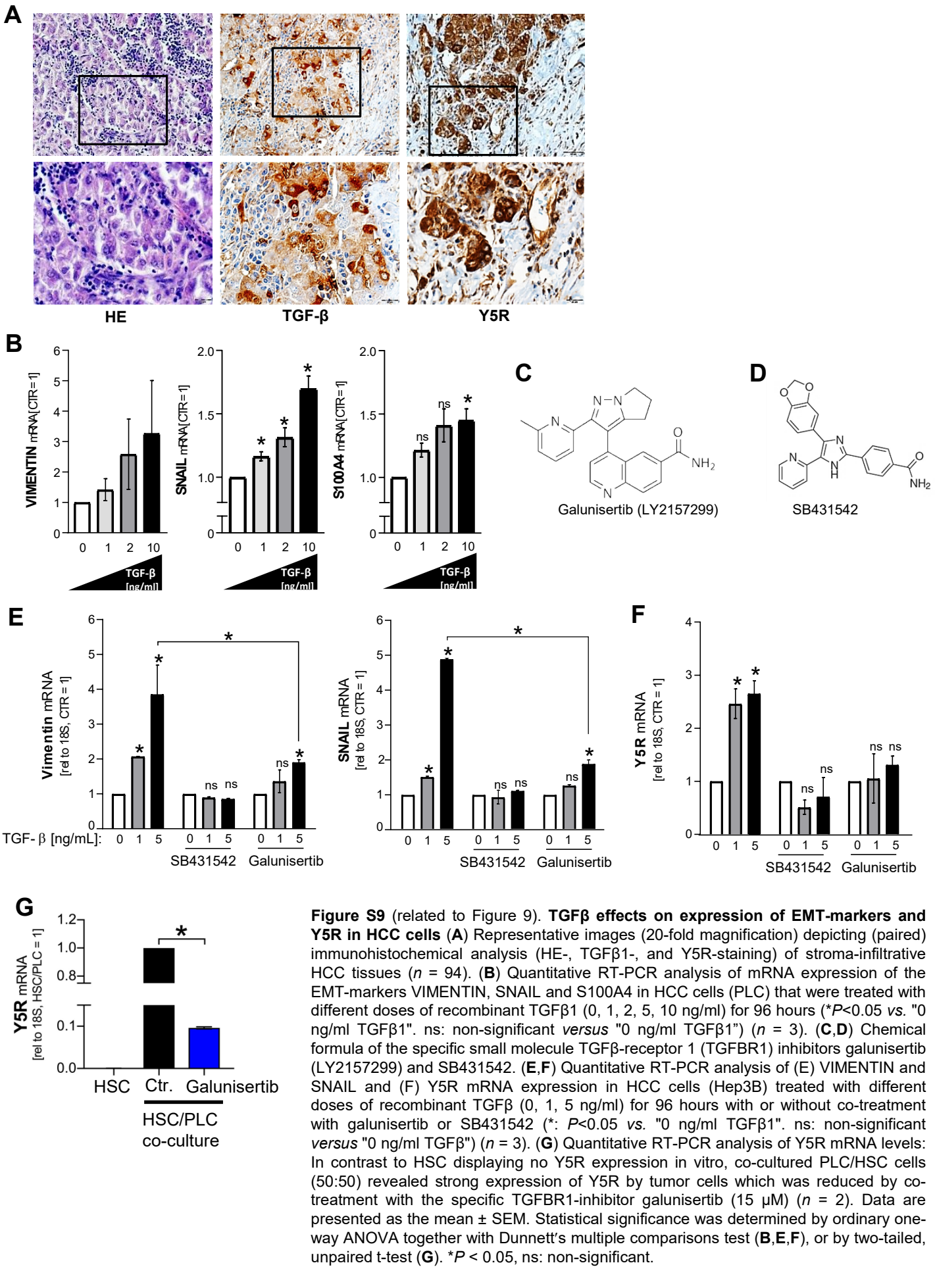

Figure S9 (related to Figure 9). **TGFβ effects on expression of EMT-markers and Y5R in HCC cells** (**A**) Representative images (20-fold magnification) depicting (paired) immunohistochemical analysis (HE-, TGFβ1-, and Y5R-staining) of stroma-infiltrative HCC tissues (*n* = 94). (**B**) Quantitative RT-PCR analysis of mRNA expression of the EMT-markers VIMENTIN, SNAIL and S100A4 in HCC cells (PLC) that were treated with different doses of recombinant TGFβ1 (0, 1, 2, 5, 10 ng/ml) for 96 hours (*P<0.05 *vs.* "0 ng/ml TGFβ1". ns: non-significant *versus* "0 ng/ml TGFβ1") (*n* = 3). (**C**,**D**) Chemical formula of the specific small molecule TGFβ-receptor 1 (TGFBR1) inhibitors galunisertib (LY2157299) and SB431542. (**E**,**F**) Quantitative RT-PCR analysis of (E) VIMENTIN and SNAIL and (F) Y5R mRNA expression in HCC cells (Hep3B) treated with different doses of recombinant TGFβ (0, 1, 5 ng/ml) for 96 hours with or without co-treatment with galunisertib or SB431542 (*: P<0.05 *vs.* "0 ng/ml TGFβ1". ns: non-significant *versus* "0 ng/ml TGFβ") (*n* = 3). (**G**) Quantitative RT-PCR analysis of Y5R mRNA levels: In contrast to HSC displaying no Y5R expression in vitro, co-cultured PLC/HSC cells (50:50) revealed strong expression of Y5R by tumor cells which was reduced by co-treatment with the specific TGFBR1-inhibitor galunisertib (15 μM) (*n* = 2). Data are presented as the mean ± SEM. Statistical significance was determined by ordinary one-way ANOVA together with Dunnett's multiple comparisons test (**B**,**E**,**F**), or by two-tailed, unpaired t-test (**G**). *P < 0.05, ns: non-significant.

Figure S9 *(continuation)*

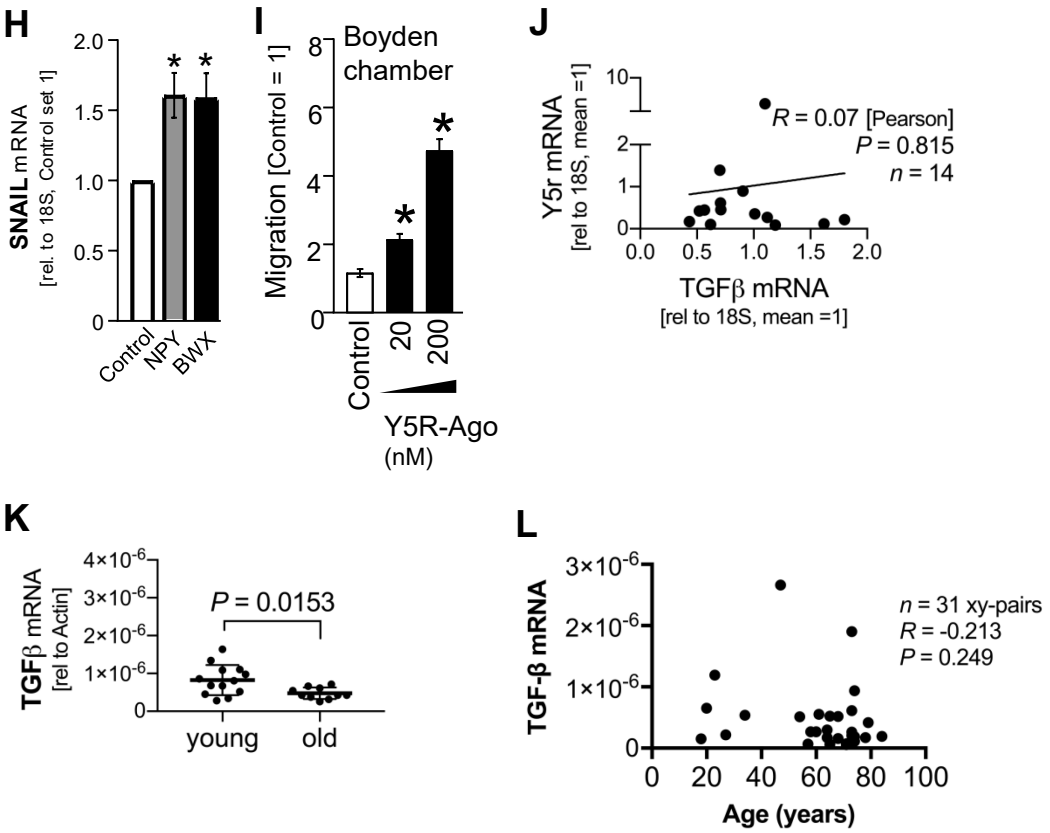

Figure S9 (related to Figure 9) (*continuation*). (**H**) SNAIL mRNA expression (qRT-PCR) in HCC cells (PLC) that were treated with recombinant NPY or the specific synthetic Y5R-agonist "BWX46" (BWX) as compared to control-treated cells (**P*<0.05 *vs.* control) (*n* = 3). (**I**) Non-directed migration (i.e. "chemokinesis") (Boyden chamber) of HCC cells (directly) treated with the specific Y5R-agonist "BWX46" (*: *P*<0.05 *vs.* control) (*n* = 3). (**J**) Pearson correlation analysis of paired Y5r and TGFβ (*n* = 14) mRNA expression (qRT-PCR) levels in peri-tumorous livers of aged C3H mice and. (**K**) TGFβ (*n* = 14) mRNA expression (qRT-PCR) levels in peri-tumorous livers of young (*n* = 13) as compared with aged (*n* = 14) C3H mice. (**L**) Paired TGFβ mRNA expression levels as quantified by qRT-PCR as correlated with age analysis in human peri-tumorous liver tissues (*n* = 31). Data are presented as the mean ± SEM. Statistical significance was determined by by ordinary one-way ANOVA together with Dunnett's multiple comparisons test (**H**,**I**), Pearson correlation analysis (**J**,**L**), and by 2-tailed, unpaired t-test (**K**). **P* < 0.05.

Figure S10

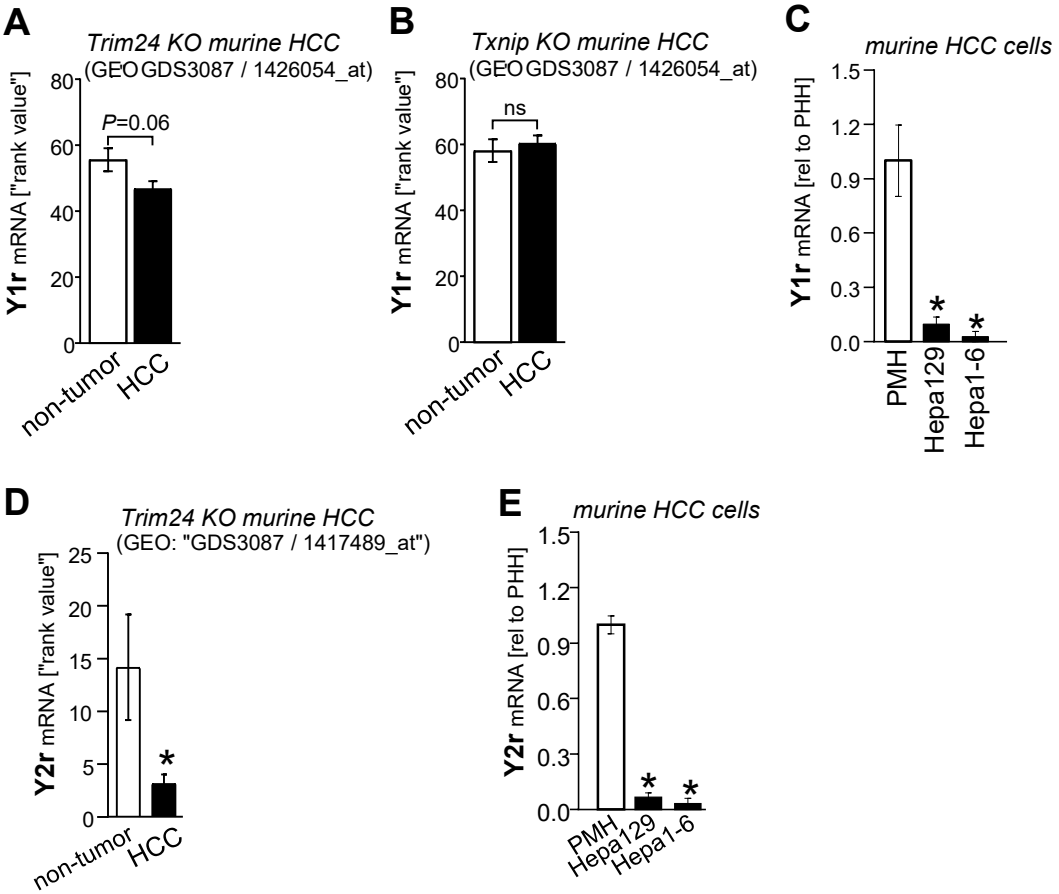

Figure S10. **Y1- and Y2-receptor subtypes do not reveal oncogenic functions in HCC and Y5R-activation is augmented by dipeptidylpeptidase 4 overexpression in HCC.** (**A**,**B**) Gene Expression Omnibus (GEO) derived datasets revealed that Y1r expression tends to be downregulated (A) (non-tumor: *n* = 5; HCC: *n* = 5) or is not regulated (B) (non-tumor: *n* = 6; HCC: *n* = 9) in HCC as compared to non-tumorous liver tissues in two established in vivo models (Trim24-knockout; Txnip-knockout) of experimental murine HCC. ns: non-significant. (**C**) Quantitative RT-PCR analysis of Y1r mRNA levels in primary murine hepatocytes (PMH) (*n* = 2) as compared with murine HCC cell lines (Hepa1-6 (*n* = 2), Hepa129 (*n* = 4)) reveals downregulation of Y1r in HCC cells (*: *P*<0.05 *vs.* PMH). (**D**) A Gene Expression Omnibus (GEO) derived dataset revealed that Y2r is downregulated in HCC (*n* = 5) as compared to non-tumorous liver tissue (*n* = 5) in an *in vivo* model (Trim24-knockout) of experimental murine HCC (*: *P*<0.05 *vs.* non-tumor). (**E**) Quantitative RT-PCR analysis of Y2r mRNA levels in primary murine hepatocytes (PMH) (*n* = 2) as compared with murine HCC cell lines (Hepa1-6 (*n* = 2), Hepa129 (*n* = 4)) reveals downregulation of Y2r in HCC cells (*: *P* < 0.05 vs. PMH). Data in are presented as the mean ± SEM. Statistical significance was determined by 2-tailed, unpaired t-test.

Figure S10 *(continuation)*

F

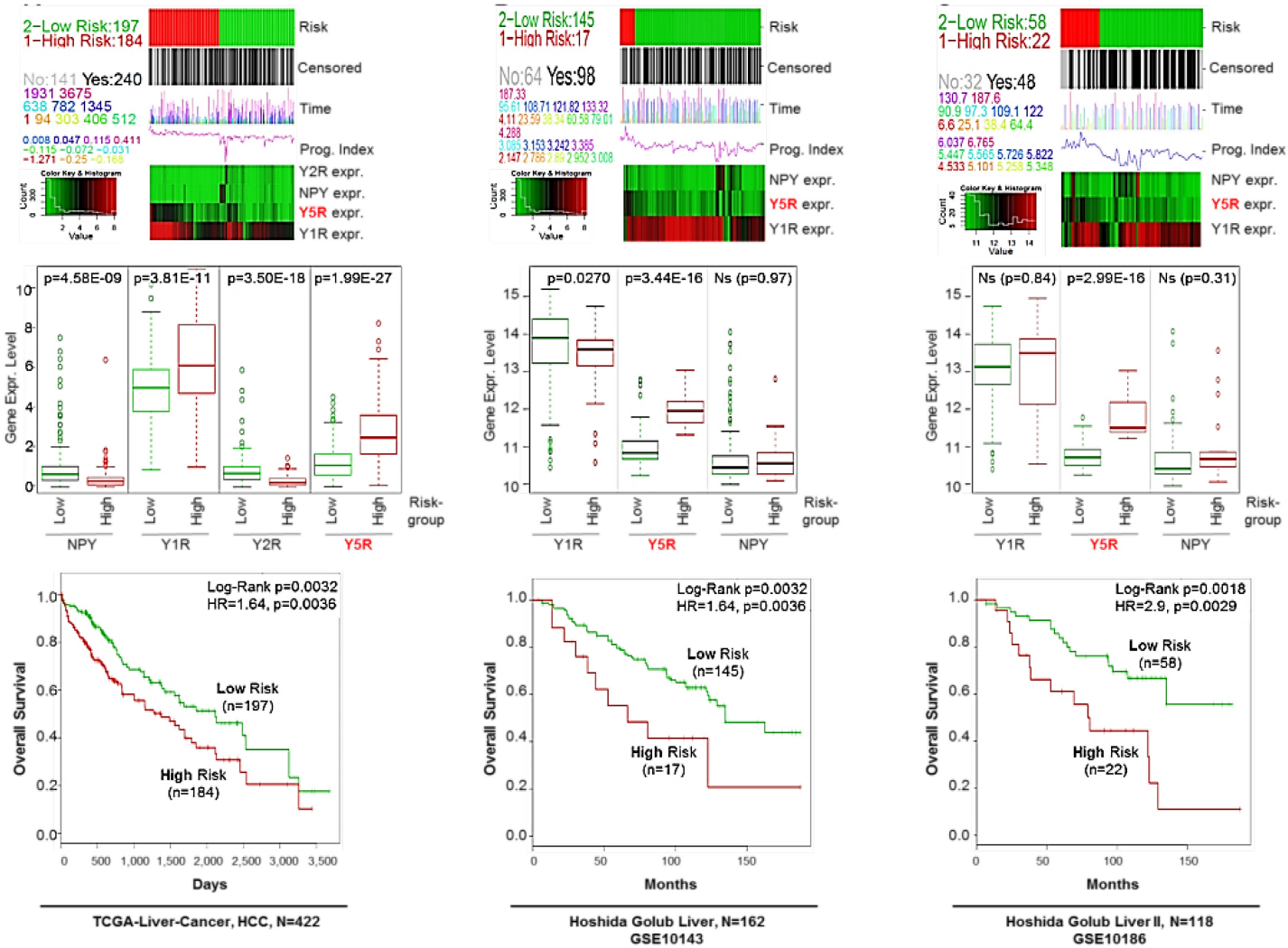

Figure S10 (*continuation*). (**F**) "SurvExpress-Biomarker validation for cancer gene expression" database analysis of combined Y5R, Y1R, Y2R and NPY expression, respectively, and according Kaplan-Meier curve for overall survival using several TCGA- and GSE-derived patient cohorts. Computational stratification into "low risk" and "high risk" patient groups was based on prognostic index ("HR": Hazard ratio). The numbers of patients in groups (*n*) are depicted within the panels. These overall survival analysis revealed that Y5R (compared with Y1R and Y2R) serves as the only oncogenic candidate target gene in HCC. Statistical significance was determined computational log-rank testing and Hazard ratios.

Figure S10 *(continuation)*

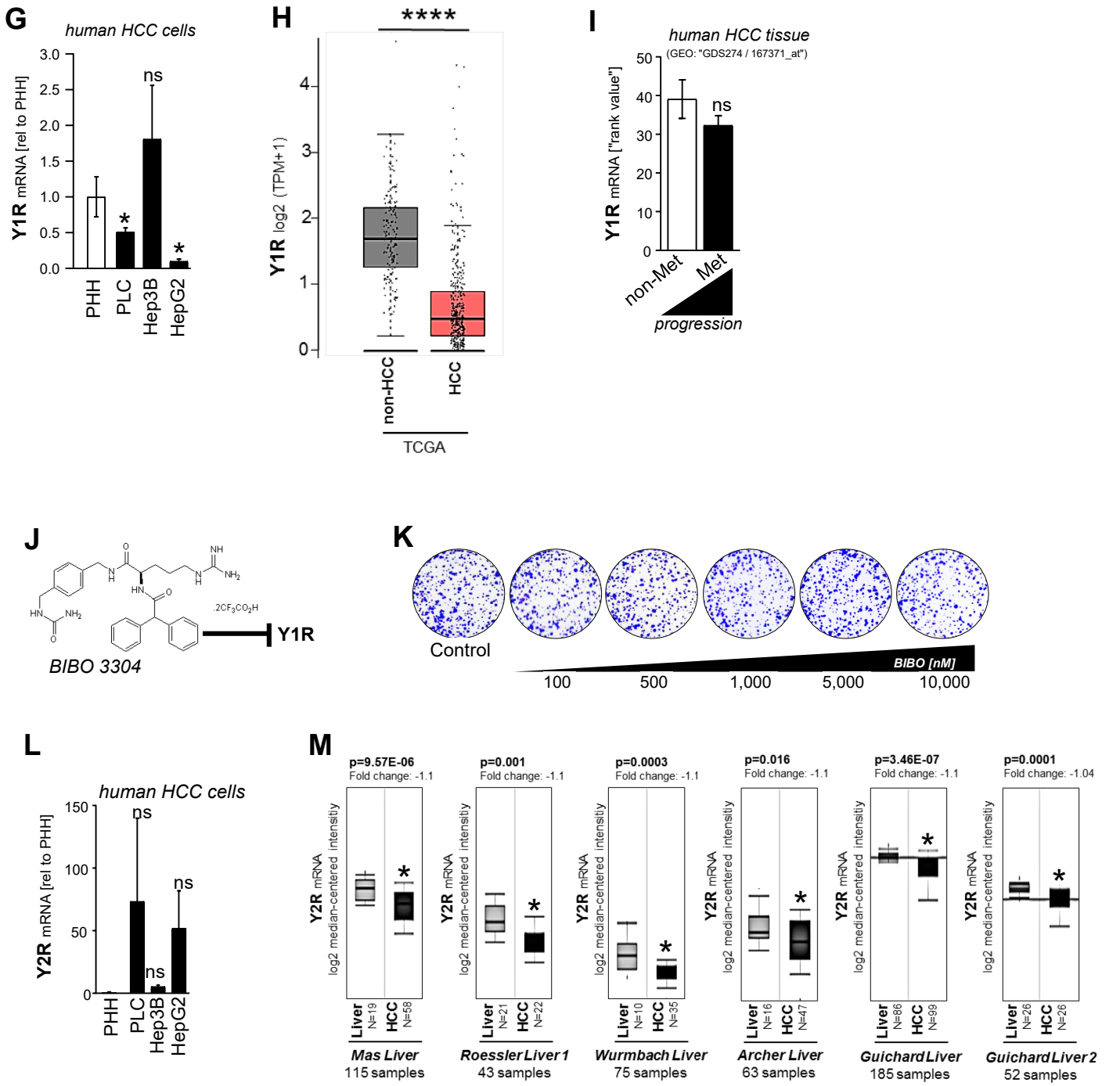

Figure S10 (*continuation*). (**G**) Quantitative RT-PCR analysis of Y1R mRNA levels in primary human hepatocytes (PHH) (n = 2) compared with human HCC cell lines (PLC (*n* = 3), Hep3B (*n* = 2), HepG2 (*n* = 2)). (**H**) Y1R expression levels in HCC tissues (*n* = 369) compared with non-tumorous liver tissues (*n* = 160) (TCGA dataset analysis) applying the Gene Expression Profiling Interactive Analysis (GEPIA) database (http://gepia.cancer-pku.cn/index.html) (Tang, Z. et al. (2017) GEPIA: a web server for cancer and normal gene expression profiling and interactive analyses. Nucleic Acids Res, 10.1093/nar/gkx247). The differential analysis is based on the selected datasets ("TCGA tumors vs TCGA normal + GTEx normal" or "TCGA tumors vs TCGA normal"). The method for differential analysis is one-way ANOVA, using disease state (Tumor or Normal) as variable for calculating differential expression: Gene expression ~ disease state. The expression data are first $\log_2$(TPM+1) transformed for differential analysis and the $\log_2$FC is defined as median(Tumor) - median(Normal). (**I**) Gene Expression Omnibus (GEO) derived analysis of of RNA levels of metastatic (*n* = 65) as compared to non-metastatic (*n* = 22) human HCC tissues. Y1R tended to be downregulated in human HCC cell lines compared to hepatocytes (G), HCC tissues as compared with matched non-tumorous liver tissues (H) and did not correlate with HCC progression (I) (*: *P* < 0.05 *vs.* PHH. ns: non-significant *versus* PHH or non-Met, respectively). (**J**,**K**) Chemical formula of the specific small molecule Y1R-inhibitor "BIBO 3304" (BIBO) (J) and clonogenicity assay (representative images) (*n* = 3) (K) of human HCC cells (e.g. PLC) treated with low and high doses of BIBO (0, 100, 500, 1,000, 5,000, 10,000 nM). (**L**) Quantitative RT-PCR analysis of Y2R mRNA levels in primary human hepatocytes (PHH) compared with human HCC cell lines (PLC, Hep3B, HepG2) (*n* = 3) (ns: non-significant *vs.* PHH). (**M**) Y2R expression levels in HCC as compared to non-tumorous liver tissues in diverse patient datasets ("*Mas Liver*", "*Roessler Liver 1*", "*Guichard Liver*", "*Guichard Liver2*", "*Wurmbach Liver*", "*Archer Liver*") using the OncomineTM database (*: *P*<0.05 *vs.* non-HCC ("Liver")). Data in are presented as the mean ± SEM. Statistical significance was determined by 2-tailed, unpaired t-test (**G**,**I**,**L**,**M**) and one-way ANOVA (**H**).

Figure S10 *(continuation)*

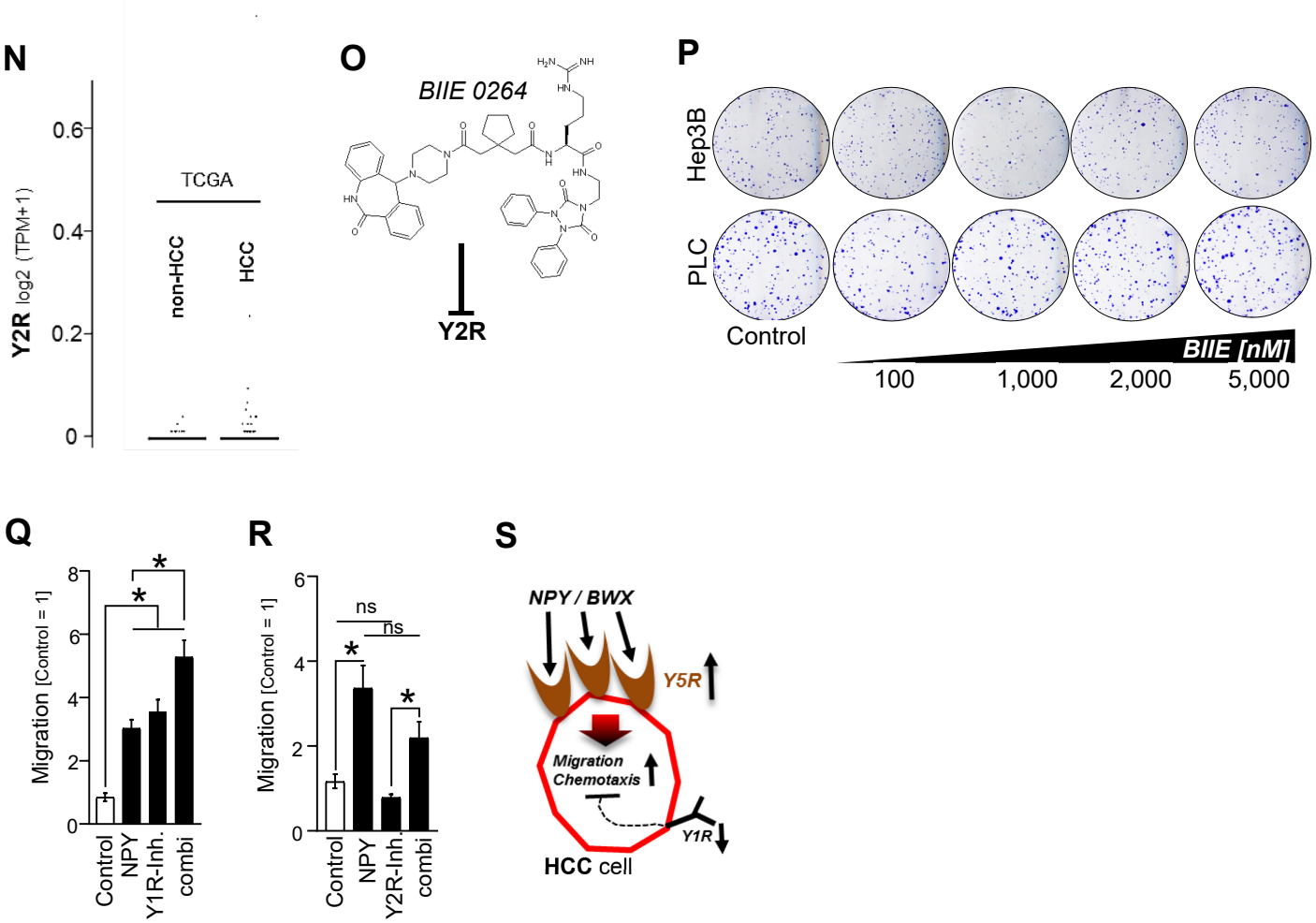

Figure S10 (*continuation*). (**N**) Y2R expression levels in HCC tissues (*n* = 369) compared with non-tumorous liver tissues (*n* = 160) (TCGA dataset analysis) applying the Gene Expression Profiling Interactive Analysis (GEPIA) database (http://gepia.cancer-pku.cn/index.html) (Tang, Z. et al. (2017) GEPIA: a web server for cancer and normal gene expression profiling and interactive analyses. Nucleic Acids Res, 10.1093/nar/gkx247). The differential analysis is based on the selected datasets ("TCGA tumors vs TCGA normal + GTEx normal" or "TCGA tumors vs TCGA normal"). The method for differential analysis is one-way ANOVA, using disease state (Tumor or Normal) as variable for calculating differential expression: Gene expression ~ disease state. The expression data are first $\log_2$(TPM+1) transformed for differential analysis and the $\log_2$FC is defined as median(Tumor) - median(Normal). This TCGA-dataset analysis confirmed very low expression levels of Y2R in HCC and non-tumorous liver tissues in accordance with qRT-PCR and Oncomine-database analysis (L,M). (**O**,**P**) Chemical formula of the specific small molecule Y2R-inhibitor "BIIE 0264" (BIIE) (O) and clonogenicity assays (exemplary images) (*n* = 3) (P) of human HCC cells (Hep3B, PLC) treated with low and high doses of BIIE (0, 100, 1,000, 5,000 nM). (**Q-S**) Boyden chamber cell migration analysis of human HCC cells (PLC) using recombinant NPY (supplemented to the lower chamber) with or without co-treatment using the specific small molecule Y1R- (BIBO) (Q, *n* = 2, replicate values) or Y2R-inhibitors (BIIE) (R, *n* = 5). Inhibition of Y1R (which was found to be downregulated in human and murine HCC) even enhanced non-directed migration of HCC cells and NPY-mediated chemotaxis significantly (Q), while inhibition of Y2R revealed no effects (R). These findings are in accordance with *i)* downregulation of NPY in cancer cells (because non-directed migration is enhanced by low local NPY concentrations and chemotaxis is induced by a gradient towards peri-tumor NPY), *ii)* downregulation of "non-Y5-NPY-receptors" (e.g. Y1R which could mediate anti-migrative effects), and *iii)* strong expression of NPY by peri-tumoral hepatocytes (induction of a gradient towards the "non-tumor site" which induces chemotaxis) (S). Most likely because of the marked overexpression of Y5R, the net effect of NPY on (directed) chemotaxis was always positive (even when applying high doses) (*P < 0.05. ns: non-significant). Data in are presented as the mean ± SEM. Statistical significance was determined by ordinary one-way ANOVA together with Dunnett's multiple comparisons test (**N**,**Q**,**R**).

Figure S11

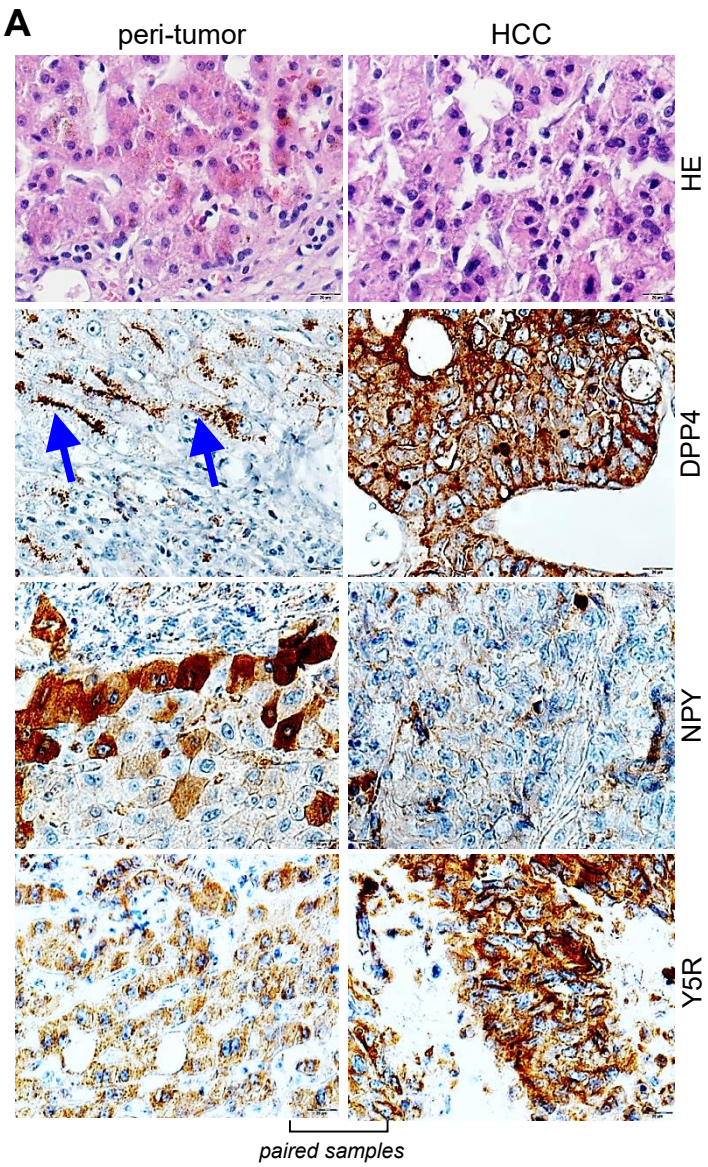

Figure S11 (related to Figures 10 and 11). (**A**) Immunohistochemical analysis (representative images of paired human HCC and peri-tumorous liver tissue) of DPP4 expression (*n* = 213) applying a tissue micro array (the black arrows depict DPP4 expression by non-tumorous hepatocytes which was mainly localized to the bile canalicular surface as described previously). Paired HE-, NPY-, and Y5R staining are also shown for the exemplary sample.

Figure S11 *(continuation)*

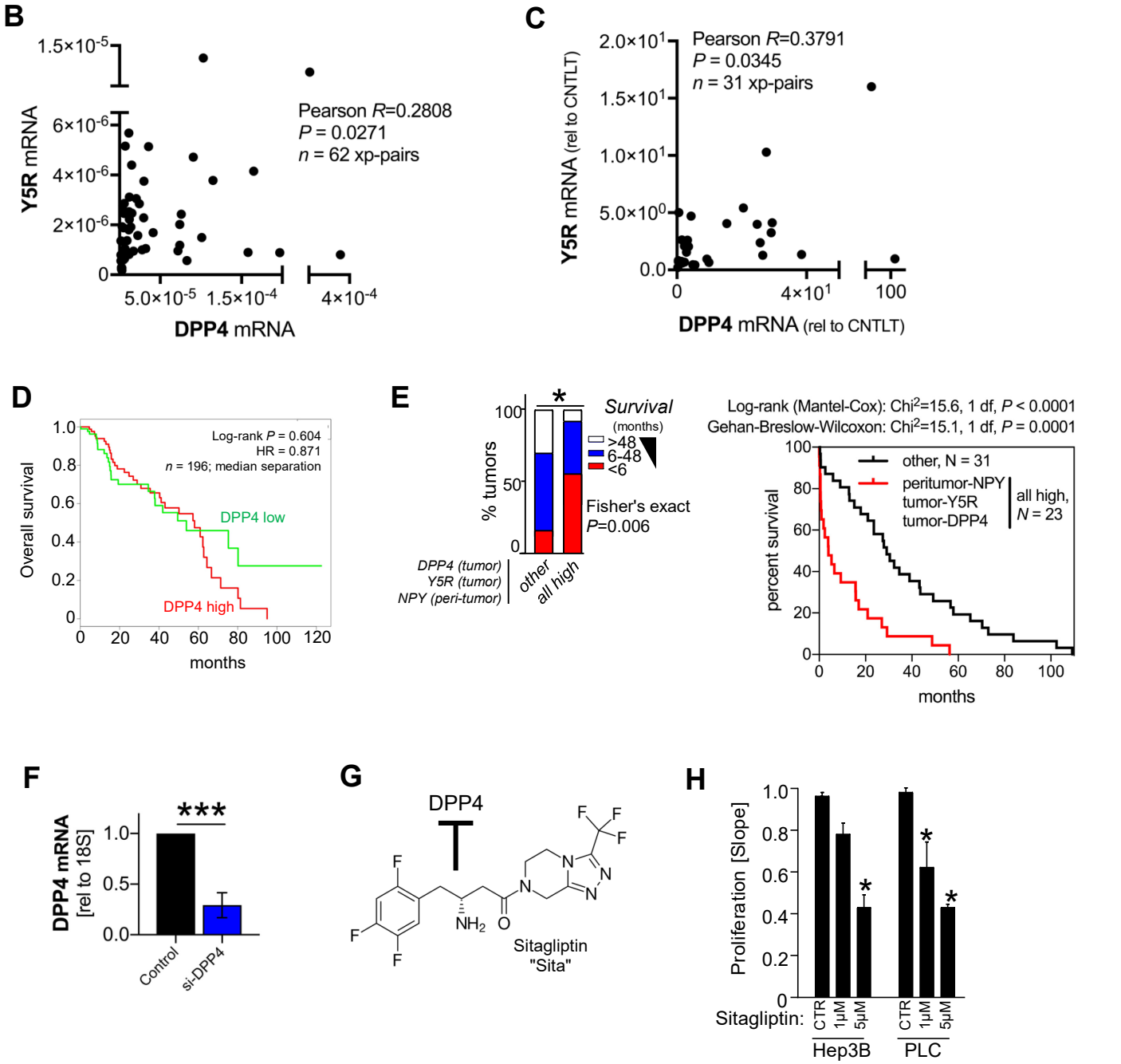

Figure S11 (related to Figures 10 and 11) (*continuation*). (**B**) Correlation of Y5R and DPP4 (n = 62) mRNA expression levels as quantified by quantitative RT-PCR applying human peri-tumorous liver tissues and corresponding HCC tissue samples. (**C**) Correlation of Y5R and DPP4 mRNA expression levels in humane HCC tissue samples (normalized to corresponding non-tumorous liver tissues) (n = 31). (**D**) "KM-express" database (http://ec2-52-201-246-161.compute-1.amazonaws.com/kmexpress/index.php) analysis of overall survival (Kaplan-Meier curve) in HCC patients with low as compared to high DPP4 expression (n = 191, median separation) applying a TCGA-derived dataset. (**E**) Immunohistochemical analysis of survival in patients combined enhanced expression of tumorous DPP4 and Y5R as well as enhanced peri-tumorous NPY expression (n = 23) compared with "other" (n = 31) conditions applying a human tissue micro array and according Kaplan-Meier curves. (**F**) Summarized DPP4 mRNA expression levels in HCC cells (PLC (n =2) and Hep3B (n = 3)) after si-RNA-mediated DPP4-knockdown as compared with control-treated cells. (**G**) Chemical formula of the specific small molecule DPP4-inhibitor sitagliptin ("Sita"). (**H**) Real-time cell proliferation (xCELLigence) analysis of HCC cells (Hep3B, PLC) in serum (i.e. NPY)-containing culture media and treatment with different doses of sitagliptin as compared with control-treated cells (CTR). Data in are presented as the mean ± SEM. Statistical significance was determined by Pearson correlation (**B,C**), two-sided Fisher′s exact test, Spearman correlation and log-rank testing (**D**,**E**), and by 2-tailed, unpaired t-test (**F,H**).

Table S0. Clinicopathological characteristics of tissue micro array samples.

Clinico-pathological feature	Categorisation	*n* (%)
Age at diagnosis		
	<65 years	81 (52.6)
	≥65 years	71 (46.1)
	nd	2 (1.3)
	total	154 (100)
Gender		
	Female	22 (14.3)
	Male	130 (84.4)
	nd	2 (1.3)
	total	154 (100)
Fibrosis (Desmet score)		
	1	10 (6.5)
	2	25 (16.2)
	3	57 (37.0)
	4	7 (4.5)
	nd	55 (35.7)
	total	154 (100)
Aetiology		
	Alcohol	52 (33.8)
	HCV	8 (5.2)
	HBV	8 (5.2)
	others (HIV, NAFLD, nd)	86 (55.8)
	total	154 (100)
Histological grade		
	G1	56 (36.4)
	G2	77 (50.0)
	G3	19 (12.3)
	nd	2 (1.3)
	total	154 (100)
Tumor stage		
	pT1	52 (33.8)
	pT2	44 (28.6)
	pT3	48 (31.2)
	pT4	5 (3.2)
	nd	5 (3.2)
	total	154 (100)
Tumor size		
	<5 cm	77 (50.0)
	≥5 cm	53 (34.4)
	nd	24 (15.6)
	total	154 (100)
Survival (months)		
	>48	12 (7.8)
	6-48	32 (20.8)
	<6	23 (14.9)
	nd	87 (56.5)
	total	154 (100)

nd: not determined / missing

Table S1. Gene expression in paired peri-HCC vs. HCC patient tissues.

Gene name	IR	*n* (%)	peri-HCC	HCC	*P**	*R*** *P***
Y5R						
	Low (score 0-1)	123 (53.2)	97	26	**<0.0001**	**0.716**
	High (score 2-3)	108 (46.8)	12	96		**<0.0001**
NPY						
	Low (score 0-1)	134 (58.0)	36	98	**<0.0001**	**-0.549**
	High (score 2-3)	97 (42.0)	80	17		**<0.0001**
TGFβ						
	Low (score 0-1)	140 (63.9)	41	99	**<0.0001**	**-0.549**
	High (score 2-3)	79 (36.1)	64	15		**<0.0001**
DPP4						
	Low (score 0-1)	131 (61.5)	97	34	**<0.0001**	**0.530**
	High (score 2-3)	82 (38.5)	8	74		**<0.0001**

*Fisher‘s exact test (two-sided); bold face representing *P*-values <0.001. **Spearman correlation (*R*) and according *P*-value (*P*). IR, immunoreactivity. Y5R, NPY, TGFβ and DPP4 staining scores were analyzed qualitatively according to both staining intensity (describing "no" ("0"), "low" ("1"), "medium" ("2"), or "strong" ("3")) and percentage of positive cells ("0": <5 %; "1": 5-20%; "2“: 20-40%, “3“:>40% positive cells).

Table S2. Clinicopathological characteristics and Y5R immunoreactivity in human HCC tissues.

Clinico-pathological characteristic	Categorisation	Y5R IR – tumor site				
		n (%)	low (score 0-1)	high (score 2-3)	*P**	*R*** *P***
Age at diagnosis	<65 years	65 (54.2)	11	54	0.266	0.054
	≥65 years	55 (45.8)	15	40		0.566
Gender	Female	14 (11.7)	2	12	0.732	-0.059
	Male	106 (88.3)	23	83		0.732
Fibrosis (Desmet score)	1	10 (11.0)	7	3	**0.006**	**0.304**
	2	22 (24.2)	5	17		**0.003**
	3	53 (58.2)	10	43		
	4	6 (6.6)	0	6		
Aetiology	Alcohol	45 (37.2)	6	39	0.184	0.190
	HCV	5 (4.1)	1	4		0.040
	HBV	6 (5.0)	0	6		
	others (HIV, NAFLD, ND)	65 (53.7)	18	47		
Tumor stage	pT1	44 (37.6)	14	30	**0.004**	**0.289**
	pT2	35 (29.9)	10	25		**0.002**
	pT3	33 (28.2)	1	32		
	pT4	5 (4.3)	0	5		
Histological grade	G1	44 (36.7)	10	34	0.949	0.032
	G2	61 (50.8)	12	49		0.752
	G3	15 (12.5)	3	12		
Survival (months)	>48	11 (19.6)	8	3	**0.002**	**-0.435**
	6-48	27 (48.2)	7	20		**0.001**
	<6	18 (32.2)	2	16		
Tumor size	<5 cm	64 (62.1)	18	7	0.344	0.115
	≥5 cm	39 (37.9)	7	32		0.344
Peri-tumor NPY IR	low (score 0-1)	35 (34.0)	14	21	**0.006**	**0.283**
	high (score 2-3)	68 (66.0)	10	58		**0.006**
Peri-tumor TGFβ IR	low (score 0-1)	34 (36.2)	11	23	0.150	0.196
	high (score 2-3)	60 (63.8)	8	52		0.063
DPP4 IR (HCC)	low (score 0-1)	32 (30.8)	13	19	**<0.001**	**0.286**
	high (score 2-3)	72 (69.2)	9	63		**0.003**

*Fisher‘s exact test (two-sided); bold face representing *P*-values <0.05. **Spearman correlation (*R*) and according *P*-value (*P*). IR, immunoreactivity; ND, not determined. Y5R, NPY, TGFβ and DPP4 staining scores were analyzed qualitatively according to both staining intensity (describing "no" ("0"), "low" ("1"), "medium" ("2"), or "strong" ("3")) and percentage of positive cells ("0": <5 %; "1": 5-20%; "2“: 20-40%, “3“:>40% positive cells). Fibrosis was determined applying the "Desmet" Score System. Ns: non-significant. For uni- and multivariate analysis, the SPSS Ordinal Regression procedure (PLUM; Polytomous Universal Model; Link function: Logit) was performed applying the dependent variables "stage" and "survival" to confirm independent prognostic factors. Parameter estimates (*P*-values, multivariate analysis) were as follows: Stage: Y5R IR – HCC (***P* = 0.006**); Age (ns); Gender (ns); Aetiology (ns); Grading (ns); NPY IR – peri-tumor (ns); Cirrhosis (ns). Survival: Y5R IR – HCC (***P* = 0.009**); NPY IR – peri-tumor (***P* = 0.033**); Age (ns); Gender (***P* = 0.028**); Aetiology (ns); Grading (ns); Stage (ns); DPP4 IR (ns); Cirrhosis (***P* = 0.010**).

Table S3. Clinicopathological characteristics and Y5R immunoreactivity in peri-HCC tissues.

Clinico-pathological characteristic	Categorisation	Y5R IR – peri-tumor site				
		n (%)	low (score 0-1)	high (score 2-3)	*P**	*R*** *P***
Age at diagnosis						
	<65 years	57 (52.8)	56	1	**<0.001**	**0.478**
	≥65 years	51 (47.2)	40	11		**<0.001**
Gender						
	Female	16 (14.8)	13	3	0.579	-0.041
	Male	92 (85.2)	83	9		0.685
Fibrosis (Desmet score)						
	1	10 (10.8)	10	0	0.885	0.121
	2	25 (26.9)	23	2		0.247
	3	52 (55.9)	46	6		
	4	6 (6.4)	5	1		
Aetiology						
	Alcohol	40 (37.0)	37	9	0.741	-0.092
	HCV	3 (2.8)	3	3		0.346
	HBV	4 (3.7)	4	0		
	others (HIV, NAFLD, ND)	61 (56.5)	52	0		
Peri-tumor NPY IR						
	low (score 0-1)	35 (33.3)	34	1	**0.038**	**0.245**
	high (score 2-3)	70 (66.7)	59	11		**0.014**

*Fisher‘s exact test (two-sided); bold face representing *P*-values <0.001. **Spearman correlation (*R*) and according *P*-value (*P*). IR, immunoreactivity; ND, not determined. NPY staining was analyzed qualitatively according to both staining intensity (describing "no" ("0"), "low" ("1"), "medium" ("2"), or "strong" ("3")) and percentage of positive cells ("0": <5 %; "1": 5-20%; "2“: 20-40%, “3“:>40% positive cells). Fibrosis was determined applying the "Desmet" Score System. For uni- and multivariate analysis, the SPSS Ordinal Regression procedure (PLUM; Polytomous Universal Model; Link function: Logit) was performed applying the dependent variable "age" to confirm independent factors. Parameter estimates (*P*-values, multivariate analysis) were as follows: Age: Y5R IR – HCC (ns); Y5R IR – peri-tumor (***P* = 0.006**); NPY IR – peri-tumor (ns); Age (ns); Gender (***P* = 0.020**); Aetiology (ns); Grading (ns); Stage (ns); DPP4 IR (ns); Cirrhosis (***P* = 0.043**); DPP4 IR – HCC (ns).

Table S4. Clinicopathological characteristics and NPY immunoreactivity in peri-HCC tissues.

Clinico-pathological characteristic	Categorisation	NPY IR – peri-tumor site				
		n (%)	low (score 0-1)	high (score 2-3)	*P**	*R*** *P***
Age at diagnosis						
	<65 years	60 (52.2)	19	41	0.840	0.028
	≥65 years	55 (47.8)	16	39		0.840
Gender						
	Female	17 (14.8)	5	12	1.000	-0-009
	Male	98 (85.2)	30	68		1.000
Aetiology						
	Alcohol	39 (33.9)	12	27	0.373	0.125
	HCV	6 (5.2)	0	6		0.187
	HBV	6 (5.2)	1	5		
	others (HIV, NAFLD, ND)	64 (55.7)	22	42		
Tumor stage						
	pT1	44 (38.9)	16	28	0.077	**0.186**
	pT2	31 (27.4)	13	18		**0.049**
	pT3	34 (30.2)	6	28		
	pT4	4 (3.5)	0	4		
Histological grade						
	G1	43 (37.4)	10	33	0.331	-0.138
	G2	58 (50.4)	19	39		0.150
	G3	14 (12.2)	6	8		
Survival (months)						
	>48	12 (20.7)	9	3	**0.010**	**-0.397**
	6-48	27 (46.6)	14	13		**0.003**
	<6	19 (32.7)	4	15		
α-SMA IR						
	low	29 (31.9)	19	10	**<0.001**	**0.441**
	moderate	47 (51.6)	13	34		**<0.001**
	high	15 (16.5)	1	14		
Fibrosis (Desmet score)						
	1	10 (10.3)	8	2	**<0.001**	**0.554**
	2	25 (25.8)	16	9		**<0.001**
	3	56 (57.7)	9	47		
	4	6 (6.2)	0	6		
Tumor size						
	<5 cm	66 (65.3)	24	42	0.114	0.169
	≥5 cm	35 (34.7)	7	28		0.114
TGF-β IR						
	low (score 0-1)	38 (37.6)	26	12	**<0.001**	**0.600**
	high (score 2-3)	63 (62.4)	5	58		**<0.001**
CD3 IR (peri-tumor)						
	low (score 0-1)	35 (34.3)	22	13	**<0.001**	**0.453**
	high (score 2-3)	67 (65.7)	12	55		**<0.001**
DPP4 IR (HCC)						
	low (score 0-1)	28 (29.5)	14	14	**0.018**	**0.214**
	high (score 2-3)	67 (70.5)	19	48		**0.038**

*Fisher's exact test (two-sided); bold face representing *P*-values <0.001. **Spearman correlation (*R*) and according *P*-value (*P*). IR, immunoreactivity; ND, not determined. NPY, TGFβ, αSMA and DPP4 staining scores were analyzed qualitatively according to both staining intensity (describing "no" ("0"), "low" ("1"), "medium" ("2"), or "strong" ("3")) and/or percentage of positive cells ("0": <5 %; "1": 5-20%; "2": 20-40%, "3":>40% positive cells), respectively. Fibrosis was determined applying the "Desmet" Score System. CD3 and CD8 staining was scored according to the number of positive immune cells per field applying 10-fold magnification ("0": < 5%; "1": 5-10%; "2": 10-20%, "3":>20% positive cells). For uni- and multivariate analysis, the SPSS Ordinal Regression procedure (PLUM; Polytomous Universal Model; Link function: Logit) was performed applying the dependent variables "stage" and "survival" to confirm independent prognostic factors. Parameter estimates (*P*-values, multivariate analysis) were as follows: Stage: Y5R IR – HCC (***P* = 0.006**); Age (ns); Gender (ns); Aetiology (ns); Grading (ns); NPY IR – peri-tumor (ns); Cirrhosis (ns). Survival: Y5R IR – HCC (***P* = 0.009**); NPY IR – peri-tumor (***P* = 0.033**); Age (ns); Gender (***P* = 0.028**); Aetiology (ns); Grading (ns); Stage (ns); DPP4 IR (ns); Cirrhosis (***P* = 0.010**).

Table S5. Clinicopathological characteristics and CD3 immunoreactivity in peri-HCC tissues.

Clinico-pathological characteristic	Categorisation	CD3 IR – peri-tumor site				
		n (%)	low (score 0-1)	high (score 2-3)	*P**	*R*** *P***
Peri-tumor α-SMA IR	low	30 (34.5)	22	8	**<0.001**	**0.509**
	moderate	43 (49.4)	8	35		**<0.001**
	high	14 (16.1)	2	12		
Fibrosis (Desmet score)	1	10 (11.0)	10	0	**<0.001**	**0.487**
	2	25 (27.5)	12	13		**<0.001**
	3	50 (54.9)	12	38		
	4	6 (6.6)	0	6		
Peri-tumor Y5R IR	low (score 0-1)	88 (88.0)	35	53	**0.042**	**0.228**
	high (score 2-3)	12 (12.0)	1	11		**0.025**
Peri-tumor TGF-β IR	low (score 0-1)	36 (37.5)	20	16	**0.007**	**0.339**
	high (score 2-3)	60 (62.5)	14	46		**0.001**
Peri-tumor NPY IR	low (score 0-1)	34 (33.3)	22	12	**<0.001**	**0.453**
	high (score 2-3)	68 (66.7)	13	55		**<0.001**

*Fisher‘s exact test (two-sided); bold face representing *P*-values <0.001. **Spearman correlation (*R*) and according *P*-value (*P*). IR, immunoreactivity; ND, not determined. NPY, TGFβ and Y5R staining scores were analyzed qualitatively according to both staining intensity (describing "no" ("0"), "low" ("1"), "medium" ("2"), or "strong" ("3")) and/or percentage of positive cells ("0": <5 %; "1": 5-20%; "2“: 20-40%, “3“:>40% positive cells), respectively. Fibrosis was determined applying the "Desmet" Score System. CD3 staining was scored according to the number of positive immune cells per field applying 10-fold magnification ("0": < 5%; "1": 5-10%; "2“: 10-20%, “3“:>20% positive cells).

Table S6. Clinicopathological characteristics and DPP4 immunoreactivity in HCC tissues.

Clinico-pathological characteristic	Categorisation	DPP4 IR – tumor site				
		n (%)	low (score 0-1)	high (score 2-3)	*P**	*R*** *P***
Age at diagnosis						
	<65 years	56 (52.3)	18	38	0.884	0.047
	≥65 years	51 (47.7)	16	35		0.630
Fibrosis score (Desmet)						
	1	10 (11.6)	5	5	**<0.001**	**0.405**
	2	23 (26.7)	11	12		**<0.001**
	3	47 (54.7)	7	40		
	4	6 (7.0)	0	6		
Aetiology						
	Alcohol	40 (37.4)	11	29	0.433	0.026
	HCV	3 (2.8)	1	2		0.791
	HBV	5 (4.7)	0	5		
	others (HIV, NAFLD, ND)	59 (55.1)	22	37		
Tumor stage						
	pT1	42 (40.8)	14	28	0.188	-0.045
	pT2	29 (28.2)	8	21		0.899
	pT3	29 (28.2)	9	20		
	pT4	3 (2.8)	1	2		
Histological grade						
	G1	39 (36.4)	9	30	0.662	-0.103
	G2	55 (51.4)	21	34		0.292
	G3	13 (12.2)	4	9		
Peri-tumor α-SMA IR						
	low	30 (35.3)	12	18	0.308	**0.259**
	moderate	43 (50.6)	10	33		**0.017**
	high	12 (14.1)	2	10		
Tumor size						
	<5 cm	57 (60.0)	15	42	0.492	-0.085
	≥5 cm	38 (40.0)	13	25		0.492
	nd					
Peri-tumor NPY IR						
	low (score 0-1)	33 (34.7)	14	19	**0.018**	**0.214**
	high (score 2-3)	62 (65.3)	14	48		**0.038**

*Fisher's exact test (two-sided); bold face representing *P*-values <0.001. **Spearman correlation (*R*) and according *P*-value (*P*). IR, immunoreactivity; ND, not determined. DPP4, NPY and αSMA staining scores were analyzed qualitatively according to both staining intensity (describing "no" ("0"), "low" ("1"), "medium" ("2"), or "strong" ("3")) and/or percentage of positive cells ("0": <5 %; "1": 5-20%; "2": 20-40%, "3":>40% positive cells), respectively. Fibrosis was determined applying the "Desmet" Score System.

Table S7. Clinicopathological characteristics and DPP4 immunoreactivity in peri-HCC tissues.

Clinico-pathological characteristic	Categorisation	DPP4 IR – peri-tumor site				
		n (%)	low (score 0-1)	high (score 2-3)	*P**	*R*** *P***
Age at diagnosis						
	<65 years	52 (50.0)	48	4	0.588	0.076
	≥65 years	52 (50.0)	48	4		0.588
Fibrosis score (Desmet)						
	1	10 (11.2)	10	0	0.863	0.091
	2	24 (27.0)	23	1		0.419
	3	48 (53.9)	45	3		
	4	7 (7.9)	6	1		
Aetiology						
	Alcohol	37 (35.6)	35	2	0.346	-0.064
	HCV	3 (2,9)	3	0		0.560
	HBV	4 (3.8)	3	1		
	others (HIV, NAFLD, ND)	60 (57.7)	55	5		
Survival (months)						
	>48	12 (20.3)	12	0	0.421	-0.221
	6-48	27 (45.8)	26	1		0.091
	<6	20 (33.9)	17	3		
α-SMA IR						
	low	31 (34.8)	27	4	0.655	-0.080
	moderate	43 (48.3)	41	2		0.752
	high	15 (16.9)	14	1		
Peri-tumor TGF-β IR						
	low (score 0-1)	37 (39.8)	35	2	0.196	0.055
	high (score 2-3)	56 (60.2)	50	6		0.595

*Fisher‘s exact test (two-sided); bold face representing *P*-values <0.001. **Spearman correlation (*R*) and according *P*-value (*P*). IR, immunoreactivity; ND, not determined. DPP4, TGFβ and αSMA staining scores were analyzed qualitatively according to both staining intensity (describing "no" ("0"), "low" ("1"), "medium" ("2"), or "strong" ("3")) and/or percentage of positive cells ("0": <5 %; "1": 5-20%; "2“: 20-40%, “3“:>40% positive cells), respectively. Fibrosis was determined applying the "Desmet" Score System.

Table S8. The REMARK checklist (*adapted*)

	Item to be reported
INTRODUCTION	
1	State the marker examined, the study objectives, and any pre-specified hypotheses. → **Y5R:** manuscript, pages 3, 4, 5; material & methods, page 7 → **NPY:** manuscript, pages 3, 4, 8; material & methods, page 7 → **DPP4:** manuscript, pages 3, 4, 16; material & methods, page 7
MATERIALS AND METHODS	
Patients	
2	Describe the characteristics (e.g., disease stage or co-morbidities) of the study patients, including their source and inclusion and exclusion criteria. → **Y5R:** supplemental data, tables S1, S2, S3; material & methods, page 7; manuscript, page 22 → **NPY:** supplemental data, tables S4; material & methods, page 7; manuscript, page 22 → **DPP4:** supplemental data, tables S6, S6; material & methods, page 7; manuscript, page 22
3	Describe treatments received and how chosen (e.g., randomized or rule-based). → n.d. (not relevant for this study)
Specimen characteristics	
4	Describe type of biological material used (including control samples) and methods of preservation and storage. → **Y5R:** material & methods, page 2, 3, 5, 7; manuscript, page 22 → **NPY:** material & methods, page 2, 3, 5, 7; manuscript, page 22 → **DPP4:** material & methods, page 2, 3, 5, 7; manuscript, page 22
Assay methods	
5	Specify the assay method used and provide (or reference) a detailed protocol, including specific reagents or kits used, quality control procedures, reproducibility assessments, quantitation methods, and scoring and reporting protocols. Specify whether and how assays were performed blinded to the study endpoint. → **Y5R:** material & methods, page 2, 3, 5, 7; manuscript, page 22 → **NPY:** material & methods, page 2, 3, 5, 7; manuscript, page 22 → **DPP4:** material & methods, page 2, 3, 5, 7; manuscript, page 22
Study design	
6	State the method of case selection, including whether prospective or retrospective and whether stratification or matching (e.g., by stage of disease or age) was used. Specify the time period from which cases were taken, the end of the follow-up period, and the median follow-up time. → **Y5R:** material & methods, page 7 → **NPY:** material & methods, page 7 → **DPP4:** material & methods, page 7
7	Precisely define all clinical endpoints examined. → **Y5R:** material & methods, page 2, 3, 5, 7; manuscript, page 22 → **NPY:** material & methods, page 2, 3, 5, 7; manuscript, page 22 → **DPP4:** material & methods, page 2, 3, 5, 7; manuscript, page 22
8	List all candidate variables initially examined or considered for inclusion in models. → **Y5R:** supplemental data, tables S1, S2, S3; material & methods, page 7; manuscript, page 22 → **NPY:** supplemental data, tables S4; material & methods, page 7; manuscript, page 22 → **DPP4:** supplemental data, tables S6, S6; material & methods, page 7; manuscript, page 22
9	Give rationale for sample size; if the study was designed to detect a specified effect size, give the target power and effect size. → n.d. (not relevant for this study)
Statistical analysis methods	
10	Specify all statistical methods, including details of any variable selection procedures and other model-building issues, how model assumptions were verified, and how missing data were handled. → **Y5R:** manuscript, page 23; figures & figure legends → **NPY:** manuscript, page 23; figures & figure legends → **DPP4:** manuscript, page 23; figures & figure legends

Source: McShane LM, Altman DG, Sauerbrei W, Taube SE, Gion M, Clark GM: Reporting recommendations for tumor marker prognostic studies (REMARK). *J Natl Cancer Inst* 2005; 97: 1180-1184.

Table S8. The REMARK checklist (*adapted*) (*continuation*)

11	Clarify how marker values were handled in the analyses; if relevant, describe methods used for cutpoint determination. → **Y5R:** material & methods, page 7 → **NPY:** material & methods, page 7 → **DPP4:** material & methods, page 7
RESULTS	
Data	
12	Describe the flow of patients through the study, including the number of patients included in each stage of the analysis (a diagram may be helpful) and reasons for dropout. Specifically, both overall and for each subgroup extensively examined report the numbers of patients and the number of events. → n.d. (not relevant for this study)
13	Report distributions of basic demographic characteristics (at least age and sex), standard (disease-specific) prognostic variables, and tumor marker, including numbers of missing values. → **Y5R:** supplemental data, tables S1, S2, S3; material & methods, page 7; manuscript, page 22 → **NPY:** supplemental data, tables S4; material & methods, page 7; manuscript, page 22 → **DPP4:** supplemental data, tables S6, S6; material & methods, page 7; manuscript, page 22
Analysis and presentation	
14	Show the relation of the marker to standard prognostic variables. → **Y5R:** supplemental data, tables S1, S2, S3; Figure 2 & Figure S2 and respective figure legends → **NPY:** supplemental data, tables S4 → **DPP4:** supplemental data, tables S6, S6 → **Y5R, NPY, Y1R, Y2R:** supplemental data, tables S1-S7; Figure S7 and respective figure legend
15	Present univariable analyses showing the relation between the marker and outcome, with the estimated effect (e.g., hazard ratio and survival probability). Preferably provide similar analyses for all other variables being analyzed. For the effect of a tumor marker on a time-to-event outcome, a Kaplan-Meier plot is recommended. → **Y5R:** supplemental data, tables S1, S2, S3; Figure 2 & Figure S2 and respective figure legends → **NPY:** supplemental data, tables S4 → **DPP4:** supplemental data, tables S6, S6
16	For key multivariable analyses, report estimated effects (e.g., hazard ratio) with confidence intervals for the marker and, at least for the final model, all other variables in the model. → **Y5R, NPY, Y1R, Y2R:** supplemental data, tables S1-S7; Figure S7 and respective figure legend
17	Among reported results, provide estimated effects with confidence intervals from an analysis in which the marker and standard prognostic variables are included, regardless of their statistical significance. → **Y5R:** supplemental data, tables S1, S2, S3; Figure 2 & Figure S2 and respective figure legends → **NPY:** supplemental data, tables S4 → **DPP4:** supplemental data, tables S6, S6 → **Y5R, NPY, Y1R, Y2R:** supplemental data, tables S1-S7; Figure S7 and respective figure legend
18	If done, report results of further investigations, such as checking assumptions, sensitivity analyses, and internal validation. → n.d. (not relevant for this study)
DISCUSSION	
19	Interpret the results in the context of the pre-specified hypotheses and other relevant studies; include a discussion of limitations of the study. → **Y5R:** manuscript, pages 5-8 → **NPY:** manuscript, pages 8-14 → **DPP4:** manuscript, pages 16-18
20	Discuss implications for future research and clinical value. → **Y5R, NPY, DPP4:** manuscript, pages 19-21

Source: McShane LM, Altman DG, Sauerbrei W, Taube SE, Gion M, Clark GM: Reporting recommendations for tumor marker prognostic studies (REMARK). *J Natl Cancer Inst* 2005; 97: 1180-1184.

SUPPLEMENTARY MATERIAL AND METHODS

Cell culture

The hepatocellular carcinoma (HCC) cell lines PLC (ATCC CRL-8024), Hep3B (ATCC HB-8064), HepG2 (ATCC HB-8065), and Huh-7 (ATCC PTA-4583) were described previously (1, 2). Primary human hepatocytes (PHH) were isolated and cultured as described in other studies (2, 3). The murine Hepa129 cell line originates from a *C3H/HeN* mouse and was obtained from the NCI-Frederick Cancer Research and Development Center (DCT Tumour Repository). Furthermore, the murine HCC cell line Hepa1-6 (ATCC CRL-1830) was used for expression analysis (qRT-PCR and co-immunofluorescence).

Treatment with recombinant proteins, agonists, inhibitors, and antibodies

Recombinant proteins, small molecule agonists, antagonists, and neutralizing antibodies were used as described in the results section, figures, and figure legends. Recombinant human TGF-β was purchased from R&D Systems (Minneapolis, USA). To activate Y5R, the synthetic high-affinity Y5R-specific-agonist BWX46 ("Y5R-Ago") (Tocris, Wiesbaden, Germany) and recombinant human neuropeptide Y ("NPY") (Merck, Darmstadt, Germany) were used. Recombinant NPY was previously shown to be initially N-terminally truncated by DPP4 in vitro and in vivo. This N-truncation is the rate-limiting step before other enzymes fully degrade NPY in vivo (4-7). An antibody against the NPY protein (Catalog No. "ab6173", Abcam, Cambridge, UK), was used to antagonize soluble NPY (1 in 500 dilution). For inhibition of Y5R-signaling, the selective high-affinity small molecule inhibitor CGP71683 (Tocris) ("Y5R-Inh#1") was used. It inhibits Y5R with high affinity and selectivity over other NPY-receptors (8). Moreover, MK-0557 (Cayman Chemicals, Ann Arbor, USA) ("Y5R-Inh#2"), 5RA972 (Tocris)

("Y5R-Inh#3"), and S-2367 ("Velneperit") (MedChemExpress, Sollentuna, Sweden) ("Y5R-Inh#4") were used (9, 10). Y5R-Inh#1 was the inhibitor with the highest affinity for Y5R and the most comprehensively specified information about affinity for other receptors and was therefore used in most experiments. For inhibition of Y1R, the specific small molecule inhibitor BIBO 2204 (Tocris) ("Y1R-Inh") (11) was used. For inhibition of Y2R, the specific small molecule inhibitor BIIE 0246 (Tocris) ("Y2R-Inh") (12) was used. Decitabine (5-Aza-2'-deoxycytidine) (Merck) was used as a hypomethylation-inducing DNA methyltransferase 1 (DNMT1)-activity-inhibitor. Sorafenib (BAY 43-9006) was obtained from Cayman Chemicals) and used as described previously (2). Forskolin (Merck) was used to induce cellular cAMP-levels. The TGF-β-receptor-1 (TGFBR1) inhibitor LY2157299 ("galunisertib") was obtained from Selleckchem (Houston, USA). Another established TGFBR1-inihibitor (SB43152) (Tocris) (13) was used to confirm the results. For inhibition of DPP4, the specific small molecule inhibitor sitagliptin ("Sita") was used. If appropriate, according doses of DMSO were used as controls.

Immunohistochemistry & Immunofluorescence

Immunohistochemistry and immunofluorescence analysis was performed using tissue micro arrays comprising human patient derived liver cancer tissue samples and mouse paraffin-embedded tissue sections as described before (2). The following primary antibodies were used: Anti-alpha-SMA antibody (Catalog No. "ab5694", Abcam, 1 in 500 dilution), anti-phospho-AKT antibody (Catalog No. "#9271", Cell Signaling, Frankfurt am Main, Germany; 1 in 50 dilution), anti-CD3 antibody (Catalog No. "C7930", Sigma Aldrich, Saint Louis, Missouri, USA; 1 in 1000 dilution), anti-phospho-ERK antibody (Catalog No. "#9101", Cell Signaling, Frankfurt am Main, Germany; 1 in 100 dilution), anti-Ki-67/MIB-1 antibody (Catalog No. "M7240", Dako GmbH, Hamburg,

Germany; 1 in 50 dilution), anti-Y5R antibody (Catalog No. "ab133757", Abcam; 1 in 1,000 dilution), anti-DPP4 antibody (Catalog No. "AF954", R&D Systems; 1 in 1,000 dilution), anti-DPP4 antibody (Catalog No. "ab61825", Abcam; 1 in 500 dilution), anti-NPY antibody (Catalog No. "ab6173", Abcam, 1 in 500 dilution), anti-NPY antibody (Catalog No. "ab10341", Abcam, 1 in 1,000 dilution), anti-NPY antibody (Catalog No. "BML-NA1233", Enzo Life Sciences, Farmingdale, USA; 1 in 500 dilution), anti-TGF-β1 antibody (Catalog No. "DM1047", Acris Antibodies; Herford, Germany; 1 in 100 dilution). Immunohistochemistry staining was analyzed semi-quantitatively and the according scores were established for each antibody as described (2).

RNA isolation and reverse transcription

RNA was isolated using E.Z.N.A. Micro Elute Total RNA Kit (Omega, Norcross, GA, USA) as described elsewhere (2). cDNAs of total RNA fractions were generated using SuperScript II Reverse Transcriptase Kit (Invitrogen, Groningen, Netherlands).

Analysis of mRNA-expression by quantitative RT-PCR

Quantitative RT–PCR was performed as described (2). The following primer pairs were used: 18S rRNA (5'-GCA ATT ATT CCC CAT GAA CG-3' and 5'-GGG ACT TAA TCA ACG CAA GC-3'), CD133 (5'-CAC TAC CAA GGA CAA GGC GT-3' and 5'- TCC AAC GCC TCT TTG GTC TC-3'), CyclinD1 (5'-GCC TGT GAT GCT GGG CAC TTC ATC TG-3' and 5'-TTT GGT TCG GCA GCT TGC TAG GTG AC-3'), Dpp4 (murine) (5'-TGT GAT GTG GTG TGG GCT AC-3' and 5'-AGG TGA AGT GAG GTT CTG CG-3'), DPP4 (human) (5'-TAC CAA CAC GAG CAG GCT AC-3' and 5'-TTC CCA TCA CCC TTG CTG TG-3'), E-cadherin (5'-ATC CTC CGA TCT TCA ATC CCA CC AC-3' and 5'-GTA CCA CAT TCG TCA CTG CTA CG TG-3'), IL-1β (5'-GAG CTC GCC AGT GAA ATG ATG GC-3' and 5'-CAA GCT TTT TTG CTG TGA GTC CCG-3'), IL-6 (5'-AAG CGC

CTT CGG TCC AGT TGC-3' and 5'-TGT CTG TGT GGG GCG GCT ACA-3'), Npy (murine) (5'-GTG TGT TTG GGC ATT CTG GC-3' and 5'-GGG GCG TTT TCT GTG CTT TC-3'), NPY (human) (5'-GCT AGG TAA CAA GCG ACT GGG-3' and 5'-TGG GCT GGA TCG TTT TCC AT-3'), Npy1r (murine) (5'-CAC CTG CAA CCA CAA TCT GC-3' and 5'-GAC GTC TTG GAC ACA TCC GT-3'), NPY1R (human) (5'-AAT GCT TCC CCG AGG TG TG-3' and 5'-TGG GGA AGA TCC GCT GGT AT-3'), Npy2r (murine) (5'-GGA TCT GCA TCA GGC ACA CT-3' and 5'-CGC CTT AGG TAG CAA GCC AT-3'), NPY2R (human) (5'-CTC CCT CGC CAC CAA AAC TTC-3' and 5'-GTG AAG GTG GGA GGA TCA GA GA-3'), Npy5r (murine) (5'-GGT ACA GCA AGA AGA CGG CA-3' and 5'- TTC TCG TGA GGG AAC GCT TG-3'), NPY5R (human) (5'-GGG CCT CAG GTG AAA CTC TC-3' and 5'-TCT CAA AGC AAG TGG GGA CC-3'), NPY5R_N-term. (human) (5'-AAT ACT GCT GCC ACT CGG AA-3' and 5'-GGC CAG ATT GCC TAT GAG GA-3'), TGF-β1 (human) (5'-GAG ATG GCA GGG ACT CTG ATA ACA CC-3' and 5'-AAA GTG CTA GGA TTA CAG GCG TGA GC-3'), Tgf-β1 (murine) (5'-AGG AGA CGG AAT ACA GG GC-3' and 5'-CCA CGT AGT AGA CGA TGG GC-3'), TGF-β2 (human) (5'-TCT AGG GTG GAA ATG GAT ACA CGA ACC-3' and 5'-TGT TAC AAG CAT CAT CGT TGT CGT CG-3'), TGF-β3 (human) (5'-CCC TGA CCA TCC TGT ACT ATG TTG GG-3' and 5'-GGG TAG CCC AAA TCC CAT TGC CAC AC-3'), TGFBR1 (human) (5'-CCT TCC AAG ATT CAA CGT GGC-3' and 5'-CCA GAG CAG CCT TCA GTC AA-3'), TGFBR2 (human) (5'-TTT GAG GAC CAG TGT TCC CG-3' and 5'-AGT AGA TGG TGG GGC AAT CG-3'), TNF-α (human) (5'-TCA CCC ACA CCA TCA GCC GCA-3' and 5'-GGG AAG GTT GGA GTG GCG TCC-3'), S100A4 (human) (5'-GGG CAA AGA GGG TGA CAA GT-3' and 5'-GCT GCT TAT CTG GGA AGC CT-3'), SNAIL (human) (5'-AGG CCC TGG CTG CTA CA AG-3' and 5'-ACA TCT GAG TGG GTC TGG AG-3'), VIMENTIN (human) (5'-AGG AAA TGG CTC GTC ACC TTC GTG AA TA-3' and 5'-GGA GTG TCG GTT GTT AAG AAC TAG AG CT-3').

si-RNA-mediated gene knockdown

Briefly, 2 x 10^4 cells were seeded each well in six-well plates. Transfection of HCC cell lines was performed using Lipofectamine RNAimax transfection reagent (Life Technologies, Darmstadt, Germany) as described (2). For siRNA-induced knockdown of Y5R, we used "FlexiTube_Hs_NPY5R_5" (functionally verified siRNA directed against human Y5R; Qiagen, Hilden, Germany), "FlexiTube_Mm_Npy5r_5" (functionally verified siRNA directed against murine Y5r; Quiagen), "FlexiTube_Mm_Npy5r_3" (functionally verified siRNA directed against murine Y5r; Quiagen), and "si-RNA-Pool-NPY5R" (functionally verified si-RNA-Pool against human Y5R; siTOOLs Biotech GmbH, Planegg, Germany). Si-RNA-Pools consist of siRNAs revealing efficient target gene knockdown with reduced off-target effects (14). Total RNA and protein were isolated 48-72 hours after transfection.

Western blotting

Western blotting and densitometric quantification was performed as described in detail in previous studies (2). The following primary antibodies were used: Anti-β-actin (Catalog No. "A1978", Sigma-Aldrich; 1 in 5,000 dilution), anti-phospho-ERK (Catalog No. "#9101", Cell Signaling, Frankfurt am Main, Germany; 1 in 4,000 dilution), anti-ERK (Catalog No. "#9102, Cell Signaling; 1 in 1,000 dilution), anti-phospho-AKT antibody (Catalog No. "#9271", Cell Signaling, Frankfurt am Main, Germany; 1 in 2000 dilution), anti-AKT Catalog No. "#9272", Cell Signaling, Frankfurt am Main, Germany; 1 in 2000 dilution), anti-Y5R antibody (Catalog No. "ab133757", Abcam; 1 in 30,000 dilution), anti-DPP4 antibody (Catalog No. "AF954", R&D Systems; 1 in 1,000 dilution), anti-DPP4 antibody (Catalog No. "ab61825", Abcam; 1 in 1,000 dilution), anti-NPY antibody (Catalog No. "ab6173", Abcam; 1 in 500 dilution), anti-NPY antibody (Catalog

No. "ab10341", Abcam; 1 in 1,000 dilution), anti-NPY antibody (Catalog No. "BML-NA1233", Enzo Life Sciences, Farmingdale, USA; 1 in 500 dilution).

Clonogenic assay

Clonogenic assays were performed to analyze stem cell behavior and attachment dependent colony formation and growth of cancer cells as described previously (2).

Analysis of cell proliferation

The xCELLigence System (Roche, Mannheim, Germany) for analysis of cell proliferation ("E-Plates") was used as described (2, 15). Cell cycle analysis was performed using fluorescence activated cell sorting (FACS) as described (16). Cell numbers ("cell counts") were counted after seeding of 200,000 cells in 6-wells. Ki67-positive cells were determined by immunofluorescence based detection after stimulation/treatment of cells using anti-Ki-67/MIB-1 antibody (Catalog No. "M7240", Dako GmbH, Hamburg, Germany; 1 in 50 dilution).

Analysis of cell migration and invasion

For migration assays, the xCELLigence System (Roche) ("CIM-Plates") and Boyden chamber assays were used as described previously (2, 15). For analysis of invasion, Boyden chamber filters were additionally coated with Matrigel.

Quantification of apoptosis

Fluorescence activated cell sorting (FACS) analysis and the "ApoDETECT™ ANNEXIN V-FITC KIT" (Invitrogen distributed by Life Technologies, Darmstadt, Germany) were used to quantify apoptotic cells as described (17).

Cell Toxicity Analysis and LDH quantification

Primary hepatocytes or cancer cells were seeded (80-90% confluency) and treated as depicted. At specified time points before and after treatment, images were taken using a light microscope as described (2). For quantification of lactate dehydrogenase (LDH), cell supernatants were collected and analysis was performed *using* enzymatic techniques as described elsewhere (2, 18).

NPY-ELISA

For quantification of NPY in cell protein lysates and supernatants as well as in serum samples, commercially available NPY-ELISA kits (Merck) were used according to the manufacturer's specifications.

In silico analysis

The Catalogue of Somatic Mutations in Cancer (COSMIC) database was used for detection of methylation patterns of the Y5R gene in large human HCC datasets, and the "MethHC" database (19) was used for confirmation. DNA methylation data were obtained from Illumina Infinium Human Methylation450 Beadchip from the TCGA Data Portal of different sites: promotor (position/probes: cg15586439 | cg13975625 | cg11784623 | cg21748223 | cg01002253 | cg04961466 | cg20618622 | cg08346159 | cg1034115), 200 base pair (bp) region at transcription start site (TSS) (position/probes: cg01002253 | cg04961466 | cg20618622 | cg08346159) and CpG-island (positiion/probes: cg11784623 | cg21748223 | cg01002253 | cg04961466 | cg20618622 | cg08346159 | cg10341154 | cg18438777) (n = 231). Data were analyzed applying the Catalogue of Somatic Mutations in Cancer (COSMIC) database and the MethHC database. Beta values were used for quantification of methylation levels ranging from 0 (least methylated) to 1(most methylated).

methylation level is given by beta= = Methylated probe intensity (M) / (Unmethylated probe intensity (U) + Methylated probe intensity (M) + 100). The respective gene expression values were obtained from RNA Seq RPKM (Reads Per Kilobase per Million mapped reads) values from the TCGA Data Portal (http://methhc.mbc.nctu.edu.tw/php/help.php). Gene centric regions were defined as follows: TSSs (transcription start sites) information was from RefSeq gene of UCSC and miRStart database for gene expression and microRNA expression, respectively. Promoter region was defines as from 1.5kb upstream to 0.5kb downstream of the RefSeq TSS. Enhancer regions was downloaded from the UCSC Table Browser. Using the NCBI Reference Sequence (RefSeq) gene annotation, probes were annotated into 8 gene regions (promoter, enhancer, TSS1500, TSS200, 5´UTR, 1st exon, gene body and 3´UTR). The hg19 RefSeq information was derived from UCSC CpG Island regions: CpG Island regions were defined based on UCSC criteria : CG content >50%, Obs/Exp, CpG ratio >0.60 and length >200 bps. The association between methylation level and expression level of the corresponding genes was determined by calculating Pearson correlation (http://methhc.mbc.nctu.edu.tw/php/help.php).

For further analysis of The Cancer Genome Atlas (TCGA) derived datasets, the Gene Expression Profiling Interactive Analysis (GEPIA) database (http://gepia.cancer-pku.cn/index.html) (20) was used. The expression data are first $\log_2$(TPM+1) transformed for differential analysis. Statistical significance was determined by computational log-rank testing and Hazard ratios. The method for differential gene expression analysis was one-way ANOVA.

The "SurvExpress-Biomarker validation for cancer gene expression" database was used as described previously (2, 21). The "Oncomine™ cancer microarray database" was used to analyze gene expression in diverse datasets (https://www.oncomine.org/)

as described (2). RNA expression levels were also analyzed using murine and human GEO datasets (GEO profiles) as described in detail in the "results" section and in according figure legends. The *Txnip*-deficient murine HCC model (22), and the *Trim24*-deficient murine HCC model (23) are well established.

Moreover, GEO profiles were used to compare Y5R expression level in older as compared with younger livers applying i) the GEO dataset "GDS2915" (analysis of livers of Fisher F344/N males at 32, 58, and 84 weeks of age) summarizing expression data (normalized expression value) of 32 (*n* = 15), 58 (*n* = 10) and 84 (*n* = 13) weeks old rats (rattus norvegicus) and ii) the GEO dataset "GDS4874" (analysis of livers from IQ-motif containing GTPase-activating protein 2 (IQGAP2) KOs at 6- and 24-months of age. IQGAP2 is a member of a multidomain scaffolding protein family that also includes IQGAP1 and IQGAP3.) summarizing normalized RNA expression levels in wild-type and IQGAP2-knockout (which are prone to HCC development (24)) non-/pre-tumorous mouse livers at 6 and 24 weeks of age (*n* = 3).

Analysis of age as correlated with Y5R expression applying patient-derived GEO/GSE data sets were done using "R" in combination with GEOquery (25) package provided by Bioconductor.org. Data sets were received by the GEOquery package. The datasets GSE14520 and GSE39791 were used. The gene Y5R (NPY5R) was provided on the Affymetrix platform as a single probeset ‘207400_at’, whereas on Illumina platform, there were two probesets ‘ILMN_2047914’ and ‘ILMN_1718198’ provided. As a summary of the expression for NPY5R on the Illumina platform, we calculated the average of the both probesets within each sample. The expression data (log_2) of each dataset were shown as normalized to the mean. To determine the effect of the age on the expression of Y5R we used a linear regression model.

Liver-organoids and hybrid-hepatocyte-HCC-organoids

Briefly, isolated embryonic liver cells (hepatoblasts) were embedded in Matrigel and covered with basal medium (HepatiCult™ Organoid Growth Medium (Mouse)) to initially form cysts that develop into liver organoids. Additionally, a transdifferentiation organoid culture system was used after induction of differentiation to functional hepatocytes derived from embryonic liver cells with a bi-lineage differentiation potential [19, 20]. Briefly, extrahepatic bile ducts and gallbladder were isolated from C57BL/6J mice, digested for 2 hours in PBS–EDTA and filtered through a 70-µm cell strainer. Pellets were embedded in Matrigel and cultivated for the first 7 day in basal culture medium containing: Advanced AdDMEM/F12 (Life Technologies) containing B27 (Sigma-Aldrich), 1,25µM N-acetylcysteine (Sigma-Aldrich), 50 ng/ml murine recombinant EGF (Preprotech), 50 ng/ml murine recombinant FGF10 (Preprotech), 10 mM Nicotinamide (Sigma-Aldrich), 50 ng/ml murine recombinant HGF (Peprotech), 100ng/ml rm Noggin (Preprotech), 10% R-spondin 1 home-made conditioned media and Y-27632 (10 µM, only the first 4 days). To induce transdifferentiation into hepatocytes, organoids were then changed to the following medium for a minimum of 10 days: Advanced AdDMEM/F12 (Life Technologies) containing B27 (Sigma-Aldrich), 1,25µM N-acetylcysteine (Sigma-Aldrich), 50 ng/ml murine recombinant EGF (Preprotech), 10 mM Nicotinamide (Sigma-Aldrich), 10nM DAPT (Sigma Aldrich) and 10nM Dexametason. To analyze interactions of HCC cells and surrounding hepatocytes, HCC cells were injected into the lumina of cystic liver organoids after transdifferentiation into hepatocytes was performed.

Murine orthotopic HCC allograft model

Male C3H/HeN mice (10 weeks old) were purchased from Charles River Laboratories (Sulzfeld, Germany) and were housed under specific pathogen-free and controlled

conditions (22°C, 55% humidity, 12-h day/night rhythm, free access to food and water). After 2 weeks of acclimatization a syngeneic orthotopic HCC model was applied (2), in which murine Hepa129 HCC cells were implanted into the liver of these mice. Therefore, mice were anaesthetized and laparotomy was performed. After preparation of the liver, mice were injected a cell suspension of 5µl containing 2.5 x 10^5 Hepa129 cells into the right median lobe of the liver. For pharmacologic inhibition of Y5R, the following conditions were applied: Starting on day 2 (after 24 hours), mice of the Y5R-Inh group ("CPG") received a single dose of CPG (15 mg/kg bodyweight) every 24h by intraperitoneal (i.p.) injection, while mice of the control group (CTR) received the vehicle only (ethanol + DMSO). For in vivo establishment of HCC (orthotopic mouse model) applying RNAi-mediated Y5r-knockout, Hepa129 cells were transfected with two pooled si-RNAs (containing "FlexiTube_Mm_Npy5r_3" and "FlexiTube_Mm_Npy5r_5" (for detailed information about siRNAs used for this study see section "si-RNA-mediated gene knockdown")) directed against murine Y5r to increase knockdown efficacy and specificity and to reduce off-target effects. Here, Hepa129 cells were injected after 48 hours of transfection applying the same conditions as for pharmacologic Y5R-inhibition as explained in detail above. Mice were killed seven days after tumor cell implantation by heart puncture under deep ketamine/xylazine anesthesia. Blood samples were collected and liver and tumor tissues were immediately snap-frozen and stored at -80°C or were formalin-fixed for subsequent analysis. Tumor size was assessed using a caliper, measuring a virtual ellipsoid’s principal axes and calculating its volume. All experimental protocols were approved by the Committee for Animal Health and Care of the local government, and conformed to international guidelines on the ethical use of animals.

REFERENCES to SUPPL. MATERIAL & METHODS

1. Bauer R, Valletta D, Bauer K, Thasler WE, Hartmann A, Muller M, et al. Downregulation of P-cadherin expression in hepatocellular carcinoma induces tumorigenicity. *Int J Clin Exp Pathol.* 2014;7(9):6125-32.
2. Dietrich P, Koch A, Fritz V, Hartmann A, Bosserhoff AK, and Hellerbrand C. Wild type Kirsten rat sarcoma is a novel microRNA-622-regulated therapeutic target for hepatocellular carcinoma and contributes to sorafenib resistance. *Gut.* 2018;67(7):1328-41.
3. Lee SM, Schelcher C, Demmel M, Hauner M, and Thasler WE. Isolation of human hepatocytes by a two-step collagenase perfusion procedure. *Journal of visualized experiments : JoVE.* 2013(79).
4. Wagner L, Bjorkqvist M, Lundh SH, Wolf R, Borgel A, Schlenzig D, et al. Neuropeptide Y (NPY) in cerebrospinal fluid from patients with Huntington's Disease: increased NPY levels and differential degradation of the NPY1-30 fragment. *J Neurochem.* 2016;137(5):820-37.
5. Frerker N, Wagner L, Wolf R, Heiser U, Hoffmann T, Rahfeld JU, et al. Neuropeptide Y (NPY) cleaving enzymes: structural and functional homologues of dipeptidyl peptidase 4. *Peptides.* 2007;28(2):257-68.
6. Wagner L, Kaestner F, Wolf R, Stiller H, Heiser U, Manhart S, et al. Identifying neuropeptide Y (NPY) as the main stress-related substrate of dipeptidyl peptidase 4 (DPP4) in blood circulation. *Neuropeptides.* 2016;57:21-34.
7. Wagner L, Wolf R, Zeitschel U, Rossner S, Petersen A, Leavitt BR, et al. Proteolytic degradation of neuropeptide Y (NPY) from head to toe: Identification of novel NPY-cleaving peptidases and potential drug interactions in CNS and Periphery. *J Neurochem.* 2015;135(5):1019-37.
8. Criscione L, Rigollier P, Batzl-Hartmann C, Rueger H, Stricker-Krongrad A, Wyss P, et al. Food intake in free-feeding and energy-deprived lean rats is mediated by the neuropeptide Y5 receptor. *J Clin Invest.* 1998;102(12):2136-45.
9. Turnbull AV, Ellershaw L, Masters DJ, Birtles S, Boyer S, Carroll D, et al. Selective antagonism of the NPY Y5 receptor does not have a major effect on feeding in rats. *Diabetes.* 2002;51(8):2441-9.
10. Erondu N, Gantz I, Musser B, Suryawanshi S, Mallick M, Addy C, et al. Neuropeptide Y5 receptor antagonism does not induce clinically meaningful weight loss in overweight and obese adults. *Cell Metab.* 2006;4(4):275-82.
11. Wieland HA, Engel W, Eberlein W, Rudolf K, and Doods HN. Subtype selectivity of the novel nonpeptide neuropeptide Y Y1 receptor antagonist BIBO 3304 and its effect on feeding in rodents. *Br J Pharmacol.* 1998;125(3):549-55.
12. Dumont Y, Cadieux A, Doods H, Pheng LH, Abounader R, Hamel E, et al. BIIE0246, a potent and highly selective non-peptide neuropeptide Y Y(2) receptor antagonist. *Br J Pharmacol.* 2000;129(6):1075-88.
13. Matsuyama S, Iwadate M, Kondo M, Saitoh M, Hanyu A, Shimizu K, et al. SB-431542 and Gleevec inhibit transforming growth factor-beta-induced proliferation of human osteosarcoma cells. *Cancer Res.* 2003;63(22):7791-8.
14. Hannus M, Beitzinger M, Engelmann JC, Weickert MT, Spang R, Hannus S, et al. siPools: highly complex but accurately defined siRNA pools eliminate off-target effects. *Nucleic Acids Res.* 2014;42(12):8049-61.
15. Ruedel A, Dietrich P, Schubert T, Hofmeister S, Hellerbrand C, and Bosserhoff AK. Expression and function of microRNA-188-5p in activated rheumatoid arthritis synovial fibroblasts. *Int J Clin Exp Pathol.* 2015;8(6):6607-16.
16. Arndt S, Wacker E, Li YF, Shimizu T, Thomas HM, Morfill GE, et al. Cold atmospheric plasma, a new strategy to induce senescence in melanoma cells. *Experimental dermatology.* 2013;22(4):284-9.
17. Wobser H, Dorn C, Weiss TS, Amann T, Bollheimer C, Buttner R, et al. Lipid accumulation in hepatocytes induces fibrogenic activation of hepatic stellate cells. *Cell Res.* 2009;19(8):996-1005.

18. Bergmeyer HU BE. Lactate dehydrogenase UV assay with pyruvate and NADPH. In: Bergmeyer HU, ed , et al., editors. *Methods of Enzymatic Analysis New York: Academic Press.* 1974:pp. 574–9.
19. Huang WY, Hsu SD, Huang HY, Sun YM, Chou CH, Weng SL, et al. MethHC: a database of DNA methylation and gene expression in human cancer. *Nucleic Acids Res.* 2015;43(Database issue):D856-61.
20. Tang Z, Li C, Kang B, Gao G, and Zhang Z. GEPIA: a web server for cancer and normal gene expression profiling and interactive analyses. *Nucleic Acids Res.* 2017;45(W1):W98-W102.
21. Aguirre-Gamboa R, Gomez-Rueda H, Martinez-Ledesma E, Martinez-Torteya A, Chacolla-Huaringa R, Rodriguez-Barrientos A, et al. SurvExpress: an online biomarker validation tool and database for cancer gene expression data using survival analysis. *PLoS One.* 2013;8(9):e74250.
22. Sheth SS, Bodnar JS, Ghazalpour A, Thipphavong CK, Tsutsumi S, Tward AD, et al. Hepatocellular carcinoma in Txnip-deficient mice. *Oncogene.* 2006;25(25):3528-36.
23. Jiang S, Minter LC, Stratton SA, Yang P, Abbas HA, Akdemir ZC, et al. TRIM24 suppresses development of spontaneous hepatic lipid accumulation and hepatocellular carcinoma in mice. *J Hepatol.* 2015;62(2):371-9.
24. Gnatenko DV, Xu X, Zhu W, and Schmidt VA. Transcript profiling identifies iqgap2(-/-) mouse as a model for advanced human hepatocellular carcinoma. *PLoS One.* 2013;8(8):e71826.
25. Davis S, and Meltzer PS. GEOquery: a bridge between the Gene Expression Omnibus (GEO) and BioConductor. *Bioinformatics.* 2007;23(14):1846-7.